



**HAL**  
open science

## Spatial and temporal evolution of detritusphere hotspots at different soil moistures

Charlotte Védère, L. Vieublé-Gonod, Valérie Pouteau, Cyril Girardin, Claire  
Chenu, Cyril Girardin

► **To cite this version:**

Charlotte Védère, L. Vieublé-Gonod, Valérie Pouteau, Cyril Girardin, Claire Chenu, et al.. Spatial and temporal evolution of detritusphere hotspots at different soil moistures. *Soil Biology and Biochemistry*, 2020, 150, pp.107975. 10.1016/j.soilbio.2020.107975 . hal-03147774

**HAL Id: hal-03147774**

**<https://hal.inrae.fr/hal-03147774v1>**

Submitted on 11 May 2022

**HAL** is a multi-disciplinary open access archive for the deposit and dissemination of scientific research documents, whether they are published or not. The documents may come from teaching and research institutions in France or abroad, or from public or private research centers.

L'archive ouverte pluridisciplinaire **HAL**, est destinée au dépôt et à la diffusion de documents scientifiques de niveau recherche, publiés ou non, émanant des établissements d'enseignement et de recherche français ou étrangers, des laboratoires publics ou privés.

# **Spatial and temporal evolution of detritusphere hotspots at different soil moistures**

Védère Charlotte<sup>a</sup>, Vieublé Gonod Laure<sup>a</sup>, Pouteau Valérie<sup>a</sup>, Girardin Cyril<sup>a</sup>, Chenu Claire<sup>a</sup>.

<sup>a</sup> UMR Ecosys, INRAE, AgroParisTech, Université Paris-Saclay, Thiverval Grignon, 78850, France

## **Corresponding author:**

[laure.vieuble@inrae.fr](mailto:laure.vieuble@inrae.fr) (L. Vieublé Gonod)

## **E-mail addresses:**

[charlotte.vedere@inrae.fr](mailto:charlotte.vedere@inrae.fr) (C. Védère).

[valerie.pouteau@inrae.fr](mailto:valerie.pouteau@inrae.fr) (V. Pouteau)

[cyril.girardin@inrae.fr](mailto:cyril.girardin@inrae.fr) (C. Girardin)

[laure.vieuble@inrae.fr](mailto:laure.vieuble@inrae.fr) (L. Vieublé Gonod)

[claire.chenu@inrae.fr](mailto:claire.chenu@inrae.fr) (C. Chenu)

## **Highlights**

- The size of the maize residue detritusphere was a few millimetres
- Dry soil showed slower residue C transfer than wet soil
- Detritusphere size was hardly impacted by moisture content
- Residue C mineralization occurred mainly on residues rather than in adjacent soil
- Residue-degrading microorganisms in soil differed from total soil microorganisms

## **Abstract**

As a result of the heterogeneous spatial distribution of microorganisms and substrates in soil and their restricted accessibility, biodegradation occurs mainly in hotspots, such as in the detritosphere, induced by decomposing plant residues. Knowing the characteristics of the volume of soil involved in biodegradation of a given organic substrate will facilitate the understanding and prediction of biodegradation.

Our objectives were (i) to identify the volume of soil involved in the biodegradation of plant residues and (ii) to determine to what extent this volume is affected by soil moisture under diffusive conditions by monitoring the mineralization and spatio-temporal evolution of residue C and microorganisms in soil at the microbial habitat scale.

We incubated repacked soil cores with a central layer of  $^{13}\text{C}$ -labelled maize residues at three different matric potentials (-0.0031, -0.031 and -0.31 MPa). We monitored  $^{13}\text{C}$  and total C mineralization, and at different dates over 45 days of incubation, we separated soil slices with increasing distances from the residues and analysed  $^{13}\text{C}$  from the residues and the microbial community structure and its activity by PLFA and  $^{13}\text{C}$ -PLFA processing. Residue mineralization increased with increasing soil moisture. A detritosphere a few mm thick was rapidly established, with a decreasing gradient of  $^{13}\text{C}$  and total PLFAs and  $^{13}\text{C}$ -PLFAs away from the residue layer. Most  $^{13}\text{C}$  from the residues was located in the first two millimetres of the detritosphere and was not dependent on the matric potential. Residue mineralization seemed to take place mainly on the residues themselves, but increasing residue C was transferred to the surrounding soil with increasing soil moisture. Dry conditions slowed residue C transfer and favoured fungi, but residue mineralization was carried out by both bacteria and fungi.

## **Keywords**

Detritosphere,  $^{13}\text{C}$  and total microbial PLFAs, Diffusion, Biodegradation, Plant residues, Spatial heterogeneity

## **Abbreviations**

PLFAs: Phospholipid fatty acids

## 1. Introduction

Soil is a heterogeneous and complex environment with a heterogeneous spatial distribution of native and exogenous soil organic matter (OM) at different spatial scales (from m to  $\mu\text{m}$ ) (Chenu and Plante, 2006; Peth et al., 2014) as well as of microorganisms (Chenu et al., 2001; Ranjard and Richaume, 2001; Chenu and Stotzky, 2002; Raynaud and Nunan, 2014). Beare et al. (1995) defined soil as the juxtaposition of microenvironments that may harbour different microbial communities and that are characterized by contrasting physical, chemical and physico-chemical conditions. These microenvironments (rhizosphere, porosphere, detritosphere, etc.) are microbial hotspots, i.e., small volumes of soil with much faster process rates and much more intensive interactions between microorganisms and their environment than those of the average soil conditions (Kuzyakov and Blagodatskaya, 2015). The detritosphere corresponds to plant residues and soil in their vicinity where microbial activities are stimulated (Gaillard et al., 1999; Kandeler, 1999). The number of hotspots and characteristics and process rates in microbial hotspots determine process rates at the macroscale (Kuzyakov and Blagodatskaya, 2015). A new generation of soil organic carbon dynamics models explicitly takes soil spatial heterogeneity and soil structure into account to obtain relatively accurate predictions (Vogel and Roth, 2001; Monga et al., 2014; Portell et al., 2018). These models are not yet widely used because they require suitable knowledge of the spatial and temporal distribution of soil microbial hotspots (Moyano et al., 2013).

When fresh OM is added to soil, microorganisms located on the OM itself and in its vicinity are involved in its biodegradation, directly by assimilating soluble C or indirectly by producing extracellular enzymes. The detritosphere has previously been studied in incubation experiments with additions of localized organic substrates, mainly labelled complex plant residues of various biochemical qualities (sup mat, Table 1). It has been established that the

biodegradation of plant residues takes place over an area of a few millimetres around the residues under diffusive conditions (Gaillard et al., 1999; Kandeler, 1999; Gaillard et al., 2003; Poll et al., 2006) and over larger distances in advective conditions (Poll et al., 2006). Similar orders of magnitude were observed with a soluble herbicide (Pinheiro et al., 2015, 2018). Some studies considered that the thickness of the detritosphere was the maximal distance to which any of the considered variables was significantly different from its value in the bulk soil, while others defined it using a breakpoint in the gradient (Kandeler, 1999). The results also depend on the methods used. Generally, thicknesses determined from measurements of enzymatic activities were smaller than when residue-derived  $^{13}\text{C}$  or microbial abundances were quantified (Gaillard et al., 1999; Kandeler, 1999; Poll et al., 2006). Incubation conditions in these studies were variable, most of them being performed under diffusive conditions, under moisture conditions ranging from pF 1.8 (-0.0063 MPa) to pF 2.9 (-0.08 MPa). Soil moisture is a key factor modulating such transfers in soil, i.e., the diffusion or advection of soluble substrates, the diffusion of gases, and the movement and activity of microorganisms in soil (Ranjard and Richaume, 2001; Ekschmitt et al., 2008; Moyano et al., 2013; Kuzyakov and Blagodatskaya, 2015). The thickness of the detritosphere was found to increase with soil moisture (Poll et al., 2006), presumably because of facilitated diffusion of soluble compounds from the residues into the soil, but no study has been performed under dry conditions.

The objectives of this work were therefore to quantify the volumes of soil involved in the biodegradation of plant residues and to determine to what extent this volume was affected over time by soil moisture, especially when the soil moisture was low, under diffusive conditions. We hypothesized that at a low soil moisture, fungi are more adapted than bacteria because of the hyphal network that facilitates access to water and nutrients (Chowdhury et al., 2011; Reichardt et al., 2001). Thus, higher fungi/bacteria ratios should be observed at low soil

moisture and lead to an increase in the size of the detritusphere by translocation of organic matter through fungal hyphae.

To meet these objectives, soil cores constructed from size-sorted aggregates with localized additions of  $^{13}\text{C}$ -enriched maize residues were incubated under laboratory conditions at 3 different matric potentials, and the dynamics of total C and  $^{13}\text{C}$  and total and degrading microorganisms were studied at the mm-cm scales over time.

## **2. Materials and Methods**

### *2.1. Experimental site and soil sampling*

The experimental site was the long-term trial of "La Cage", based in Versailles (France), including plots managed under conservation agriculture without tillage and with a permanent plant cover (fescue or alfalfa) eliminated before the establishment of the main crop (with residue restitution at the soil surface). The soil is a Luvisol (WRB) containing  $150 \text{ g kg}^{-1}$  clay,  $173 \text{ g kg}^{-1}$  fine silt,  $303 \text{ g kg}^{-1}$  coarse silt,  $312 \text{ g kg}^{-1}$  fine sand and  $64 \text{ g kg}^{-1}$  coarse sand (Autret et al. 2016).

The soil was sampled in June 2017 from between 5 and 10 cm below the surface. The soil water content at the time of sampling was  $124 \text{ g kg}^{-1}$ . Aggregates between 2 and 5 mm in diameter were selected by sieving and stored at  $4^\circ\text{C}$  until use. This fraction of soil had a carbon content of  $13.5 \text{ g kg}^{-1}$  and a nitrogen content of  $0.95 \text{ g kg}^{-1}$ .

### *2.2. Crop residues*

Inflorescences of dry maize labelled with  $^{13}\text{C}$  ( $\delta^{13}\text{C} = 1947.1 \text{ ‰}$ ) and supplied by S.

Recous (INRAE, Reims) contained  $410 \text{ g kg}^{-1}$  carbon and  $21.2 \text{ g kg}^{-1}$  nitrogen ( $\text{C/N} = 19.6$ ). The residues were ground to particle sizes between 0.2 and 2 mm. Residues were composed of  $22.8 \pm 2.4\%$  soluble organic compounds,  $41.6 \pm 2.4\%$  hemicellulose,  $31.8 \pm 1.5\%$  cellulose and  $3.9 \pm 0.1\%$  lignin and cutin (van Soest fractioning).

### 2.3. Core design

Cores were prepared in 2 stages. First, two PVC cylinders drilled to allow for air to circulate were filled with 66.31 g (dry equivalent) of aggregates (2-5 mm) and compacted using a mechanical press at a bulk density close to that of the sampled soil, i.e.,  $1.3 \text{ g cm}^{-3}$ . The two cylinders were then stacked on each side of two stainless steel 200  $\mu\text{m}$  meshes between which the residues were placed as a homogeneous layer (sup mat Fig. 1). The cores initially contained 0.166 g of residues for 132.62 g of dry soil, i.e.,  $0.52 \text{ g C}_{(\text{residues})} \text{ kg}^{-1}$  dry soil. Each final core measured 57 mm in diameter and 40 mm in height. Control cores without residues were also produced.

Aggregates were equilibrated at three different matric potentials equivalent to pF 3.5 (-0.3 MPa, pores with neck diameters  $< 1 \mu\text{m}$  filled with water), pF 2.5 (-0.03 MPa, pores with neck diameters  $< 10 \mu\text{m}$  filled) and pF 1.5 (-0.0031 MPa pores with neck diameters  $< 100 \mu\text{m}$  filled). Water contents of aggregates were adjusted before construction of the cores for the pF 2.5 and 3.5 groups and after construction of the cores for the pF 1.5 group. The corresponding water contents at pF 2.5 and 1.5, determined from water retention curves (sup mat Fig. 2), were 251 and 426  $\text{g water kg}^{-1}$  soil, respectively. The moisture at pF 3.5 corresponded to the initial water content of the sampled soil, i.e., 124  $\text{g kg}^{-1}$  soil. The matric potential of pF 2.5 was adjusted by adding water to increase the soil moisture from 124  $\text{g kg}^{-1}$  soil to 251  $\text{g kg}^{-1}$  soil. To reach a pF of 1.5, the aggregates were placed in the cylinders on a porous pressure

plate, i.e., a chamber allowing for the application of a controlled pressure on saturated samples to adjust their matric potential (Klute, 1986), at -0.0031 MPa. This method avoided manipulating the highly deformable aggregates at pF 1.5.

Each core was then placed in a 1 L air-tight jar (equipped with a septum allowing for gas sampling) on a nylon support allowing for air circulation all around the core. The water content was kept constant, with 10 mL of water placed at the bottom of the jar and the core moisture adjusted if necessary on the basis of regular weighing. In preliminary experiments, we checked that the soil water content was similar on both sides of the residue layer throughout the incubation. The atmosphere was regularly renewed (with CO<sub>2</sub>-free air rewetted by bubbling in a water flask). The jars were incubated in the dark at 20°C for up to 45 days.

A set of 21 cores (4 cores with residues and 3 control cores without residues for each of the 3 matric potentials) was prepared for monitoring the total C and <sup>13</sup>C mineralization. For analyses of soil C contents (total and <sup>13</sup>C) and soil phospholipid fatty acids (PLFAs) (total and <sup>13</sup>C) on a mm scale, requiring destructive samples, 36 additional cores with residues were prepared with 3 replicates per matric potential and per date of analyses (4 dates). All the cores for mineralization monitoring and destructive sampling were prepared and incubated identically.

#### *2.4. Mineralization measurements*

Organic carbon mineralization was regularly monitored for 45 days, with measurements on days 1, 3, 7, 15, 21, 28, 35, 42 and 45. Total CO<sub>2</sub> was measured directly from the jars using a gas chromatograph (Agilent, 490 Micro GC System, CA, USA), and its concentration, obtained in ppm, was converted to μg C-CO<sub>2</sub> g<sup>-1</sup> dry soil following the relation:

$$(1) \text{ C-CO}_2 \text{ (total)} = (\text{CO}_2 \text{ (total-ppm)} / \text{m}_{\text{dry soil}}) \times \rho C$$



where  $\text{CO}_2$  (total-ppm) is the content of total  $\text{CO}_2$  in ppm,  $m_{\text{dry soil}}$  is the mass of dry soil of the core in g, and  $\rho_{\text{C}}$  is the density of carbon ( $0.5 \mu\text{g } \mu\text{L}^{-1}$ , according to the ideal gas law at  $20^\circ\text{C}$ ). This calculation was performed for a volume of air of 1 L.

For  $^{13}\text{C}$ - $\text{CO}_2$  measurements, gas was sampled from the jars, transferred to a glass bottle under vacuum and analysed the same day.  $^{13}\text{C}$ - $\text{CO}_2$  was measured with a gas chromatograph (5890 GC Hewlett-Packard, CA, USA) coupled with an isotopic mass spectrometer (Isochrome III, Optima, Micromass-GVI Ltd, Manchester, UK). The  $^{13}\text{C}$  signature of the residues was measured on dry, ground residue aliquots using an isotopic mass spectrometer (Precision, Elementar UK Ltd, Cheadle, UK). The measured  $\delta^{13}\text{C}$  of the atmosphere of the jars with cores containing residues ( $\delta_{\text{measured}}$ ), of the residues ( $\delta_{\text{residues}}$ ) and of the  $\text{CO}_2$  evolved from control cores ( $\delta_{\text{SOM}}$ ) were expressed in ‰ relative to Vienna Pee Dee Belemnite (VPDB), and the  $\%_{\text{residues}}\text{C}$  of each sample gas measurement was obtained using the relation:

$$(2) \quad \%_{\text{residues}}\text{C} = (\delta_{\text{measured}} - \delta_{\text{SOM}}) / (\delta_{\text{residues}} - \delta_{\text{SOM}})$$

The quantity of  $\text{C-CO}_2$  (residues) in  $\mu\text{g C-CO}_2 \text{ g}^{-1}$  dry soil was then obtained by the relation:

$$(3) \quad \text{C-CO}_2(\text{residues}) = \text{C-CO}_2(\text{total}) \times \%_{\text{residues}}\text{C}$$

## 2.5. Core slicing

To analyse the detritosphere soil, the 2 cylinders of soil constituting the cores were separated from the meshes containing the residues, and the remaining residues between the two meshes were removed and stored at  $-20^\circ\text{C}$  before lyophilization. Slices 2 mm thick were cut out of the 2 cylinders of each core from the residue bed (6.63 g of dry soil per slice). Thus, 4 samples corresponding to 0-2 mm, 2-4 mm, 4-6 mm and 12-14 mm

(as distant soil) away from the residues were obtained. The slices of the 2 cylinders corresponding to the same sampling distances were pooled to increase the soil mass available for analysis and stored at -20°C before lyophilization.

## *2.6. Analyses of <sup>13</sup>C content of residues and soil*

<sup>13</sup>C contents in residues and in the different slices of soil were analysed at different sampling times using an elemental analyser (Vario Isotope Select, Elementar, Hanau, Germany) coupled to an isotopic mass spectrometer (Precision, Elementar UK Ltd, Cheadle, UK). The <sup>13</sup>C contents of the intermediate soil slices (between 6 and 12 mm) that were not analysed were estimated by linear regression.

## *2.7. PLFAs extraction and analyses*

PLFAs analyses were carried out on the 0-2, 2-4, 4-6 and 12-14 mm soil slices after lyophilization. PLFAs were extracted according to the method described by Frostegård et al. (1993). The lipids of the microbial cell membranes were extracted after mixing the soil samples with a mixture of methanol, chloroform and citrate buffer. Then, phospholipids were separated from neutral lipids and glycolipids chromatographically on a silica column. Recovered phospholipids were depolymerized and transmethylated during alkaline methanolysis and stored at -20°C until analyses.

PLFAs were separated using a gas chromatograph with a flame ionization detector (Agilent, 6890 Plus GC, version 1.03.08, Germany). A qualitative standard mixture based on fatty acids (from C11:0 to C20:0) (BAME: bacterial acid methyl ester CP, 47080\_U, Sigma Aldrich) was used to identify PLFAs contained in the samples according to their retention

time. A second quantitative FAME standard (Supelco 37 component fame mix, CRM47885, Sigma-Aldrich) was used to generate calibration curves and quantify the PLFAs extracted from the samples. The standard nomenclature of PLFAs described in Frostegård et al. (1993) was used. Mono-unsaturated and cyclopropylated PLFAs (C16:1w7c, C18:1w9c, C18:1w9t) were considered markers of gram-negative (gram-) bacteria, iso- and anteiso-PLFAs (iC15:0, aC15:0, iC16:0) were considered gram-positive bacteria (gram+) markers, and PLFA C18:2w6c was considered a fungal marker (Quideau et al., 2016). The total microbial community (total microbial PLFAs) was expressed by the addition of gram-, gram+, and fungal markers as well as the C14:0, C15:0, C16:0 and C18:0 fatty acids obtained. The fungi/bacteria ratios (ratios of the fungal marker to the gram+, gram- C14:0 and C15:0 markers) were calculated.

## 2.8. <sup>13</sup>C-PLFAs analyses

Analysis of the isotopic composition of PLFAs was carried out on a gas chromatograph (Agilent, 6890A, USA) coupled to an Isochrom continuous flow IRMS (Isochrom-Isoprime, Micromass UK Ltd, Manchester, UK). The fatty acid retention times were determined using the BAME standard (bacterial acid methyl ester CP, 47080\_U, Sigma Aldrich) and FAME mixture (Supelco 37 component fame mix, CRM47885, Sigma-Aldrich). <sup>13</sup>C values of the methyl esters of individual fatty acids ( $\delta_{\text{measured PLFA}}$ ) were corrected to remove the value of the methyl group added during the esterification ( $\delta_{\text{methyl}} = -65 \text{ ‰}$ ) (Lerch et al., 2009) according to the following formula:

$$(4) \delta_{\text{PLFA}} = (\delta_{\text{measured PLFA}} \times (nC_{\text{PLFA}} + 1) - \delta_{\text{methyl}}) / nC_{\text{PLFA}} \text{ with } nC_{\text{PLFA}} = C \text{ number of fatty acids}$$

The measured  $\delta^{13}\text{C}$  of the PLFAs ( $\delta_{\text{PLFA}}$ ), of the residues ( $\delta_{\text{residues}}$ ) and of control PLFAs ( $\delta_{\text{control}}$ ) were expressed in ‰ relative to VPDB, which allowed for calculation of the  $\%_{\text{residues}}\text{PLFA}$  of each sample using the relation:

$$(5) \%_{\text{residues}}\text{PLFA} = (\delta_{\text{measured PLFA}} - \delta_{\text{FAME}}) / (\delta_{\text{residues}} - \delta_{\text{control}}),$$

Then, the quantity of labelled PLFAs was determined according to the following formula:

$$(6) {}^{13}\text{C-PLFA} = \text{PLFA}_{(\text{tot})} \times \%_{\text{residues}}\text{PLFA}.$$

${}^{13}\text{C-PLFAs}$  were measured only in samples incubated for 7 days at pF 1.5 and 3.5.

## 2.9. Statistical analyses

Normality of the mineralization,  ${}^{13}\text{C}$  in residues and soil, total microbial PLFAs and  ${}^{13}\text{C}$ -microbial PLFAs data sets and the homogeneity of the variances were evaluated with the Shapiro-Wilk test ( $P > 0.05$ ) and Bartlett test ( $P > 0.05$ ), respectively. When these two conditions were met, analysis of variance (ANOVA) as well as a Tukey multiple comparison test (with a confidence interval of 95%) were performed. On the other hand, when these two conditions were not satisfied, a non-parametric Kruskal-Wallis test as well as a Dunn multiple comparison test (with a confidence interval of 5%) were implemented.

Microbial PLFAs corresponding to gram-, gram+ and fungi according to the 3 different matric potentials and to the different slices of soil located at increasing distances from the residues at days 3 and 45 of incubation were compared using PCA. The structure of total and active microorganisms after 7 days of incubation were compared in the same way. Statistics were performed with RStudio version 1.1.463.

## 3. Results

### *3.1.1. Total carbon mineralization*

Total carbon mineralization increased with increasing water content (Fig. 1). Cores with residues showed a steep increase in the total carbon mineralization at the beginning of the incubation until day 10 and then a relatively slower increase until day 45, while the increase in control cores was more constant during the whole incubation period. After 45 days, mineralization was 63% greater at pF 1.5 than at pF 3.5 for control soils and 49% greater at pF 1.5 than at pF 3.5 for soil amended with residues.

### *3.1.2. Mineralization of residue-derived carbon*

Cumulative mineralization of the residues showed similar dynamics at the different matric potentials, with very rapid mineralization from the start of incubation eventually slowing down (Fig. 2a). The mineralization of residues increased with increasing moisture. After 45 days, between 33 and 46% of residue-derived C was mineralized. Residue mineralization rates (Fig. 2b) exhibited similar dynamics for the 3 water contents. Mineralization rates were maximum at approximately day 7 of incubation and then decreased rapidly to reach values equal to or lower than 0.2% for the 3 studied matric potentials at day 45 of incubation. Mineralization rates increased with increasing soil moisture only during the first 14 days of incubation.

## *3.2. The fate of residue C*

$^{13}\text{C}$  initially originating from the residues was distributed in all 3 compartments over time. A certain fraction of  $^{13}\text{C}$  persisted in residues, some was transferred into the soil, and some  $^{13}\text{C}$  was mineralized (either from the residue layer itself or after its transfer into the soil). On the scale of whole cores,  $^{13}\text{C}$  balances varied between 76.0% and 96.1% and were adjusted to 100% for comparison.

After 3 days of incubation, more than 80% of  $^{13}\text{C}$  remained concentrated in the residue layer. Only a small amount of residue C was mineralized (<10%), and that mineralized at pF 2.5 and 3.5 was significantly less than that mineralized at pF 1.5. Finally, the amount of  $^{13}\text{C}$  present in the soil was not significantly different for the 3 matric potentials and accounted for less than 10% of the total  $^{13}\text{C}$  content (Fig. 3).

The proportion of  $^{13}\text{C}$  in the residue layer relative to the amount of  $^{13}\text{C}$  initially added decreased significantly over time. Conversely, the proportion of mineralized  $^{13}\text{C}$  increased. Differences in  $^{13}\text{C}$  content in the residues and mineralized fractions were significant between pF 1.5 and 3.5 after 15 days of incubation but not between the pF 2.5 and 3.5 groups. In addition, we observed a significant correlation ( $R^2 = 0.99$ ,  $P < 0.01$ ) between the decrease in  $^{13}\text{C}$  in the residue layer and the increase in mineralized  $^{13}\text{C}$  (sup mat Fig. 3).  $^{13}\text{C}$  increased in soil at the beginning of the experiment until day 7 and was higher in high-moisture soils than in low-moisture soils after 7 days. At the end of the incubation, mineralized  $^{13}\text{C}$  represented approximately 10% of the total  $^{13}\text{C}$  (Fig. 3).

### *3.3. Transfer of residue C in the soil at the millimetre scale*

The transfer of  $^{13}\text{C}$  into the soil occurred mainly in the first 2 mm, as this distance represented approximately 80% of the total  $^{13}\text{C}$  transferred into soil regardless of the sampling

date (Fig. 4). At day 7, more  $^{13}\text{C}$  had been transferred into the soil at pF 1.5 than at pF 3.5, and the differences were significant. The quantities of  $^{13}\text{C}$  present in the soil significantly decreased with increasing distance from the residue layer, but  $^{13}\text{C}$  was detected up to 14 mm from the residues (Fig. 4). The quantities of  $^{13}\text{C}$  transferred to the 4 mm section were not significantly different for the different matric potentials. Beyond 4 mm, the amount of  $^{13}\text{C}$  present in soil was significantly higher at pF 1.5 than at pF 3.5, regardless of the date of measurement. Thus, at relatively high soil moisture contents, the  $^{13}\text{C}$  from the residues was transferred over relatively great distances in the soil.

Transfer of  $^{13}\text{C}$  into the soil was very rapid and observable within 3 days of incubation, regardless of soil moisture (there was no significant difference between the 3 pF groups). The amount of  $^{13}\text{C}$  in the soil was maximal after 7 days of incubation for the pF 1.5 groups (Fig. 4a), after 15 days for the pF 2.5 groups (Fig. 4b) and later for the pF 3.5 groups (Fig. 4c). The transfer of  $^{13}\text{C}$  in the soil was hence slower for low-moisture soils than for high-moisture soils. Based on the distribution of  $^{13}\text{C}$  observed after 3 days in the soil reaching a distance of 12 mm at pF 1.5 and 2.5, we calculated a minimum transfer rate of  $4.6 \times 10^{-6} \text{ cm}^2 \text{ s}^{-1}$ . At pF 3.5,  $^{13}\text{C}$  was quantified only up to the third section, which fixed the minimum distance reached at 4 mm, resulting in a minimum transfer rate of  $1.5 \times 10^{-6} \text{ cm}^2 \text{ s}^{-1}$ .

#### *3.4. Distribution of total microorganisms*

The initial quantities (6 days after matric potential adjustment and before the incubation started) of total microbial PLFAs in aggregates were  $11.7 \pm 0.5 \text{ nmol g}^{-1}$  soil at pF 1.5,  $11.5 \pm 0.7 \text{ nmol g}^{-1}$  soil at pF 2.5 and  $8.8 \pm 0.9 \text{ nmol g}^{-1}$  soil at pF 3.5 (significantly lower than at the other two pFs). Total microbial PLFAs decreased significantly in the soil between day 0 and day 7 but remained stable thereafter (sup mat Fig. 4a). All dates combined, total

microbial PLFAs were greater at pF 3.5 than at pF 1.5 and 2.5 (sup mat Fig. 4b). The differences were significant after 7 days of incubation. Total microbial PLFAs were significantly higher near the residues than at greater distances (sup mat Fig. 4c). Gradients were more marked at pF 1.5 and 2.5 than at pF 3.5, where PLFAs were more homogeneously distributed in soil.

After 3 days of incubation, microbial communities were similar for the 3 pF groups (Fig. 5a) but were different between the 2 mm of soil adjacent to residues and the more distant soil, with significantly more fungi and gram- and gram+ bacteria in the vicinity of residues (Fig. 5c). After 45 days of incubation, the difference between microbial communities was greater between groups at pF 3.5 and at the two other matric potentials with significantly more fungi and gram- bacteria at pF 3.5 (Fig. 5b). Microbial communities were different between the first 2 mm and the rest of the soil, with significantly more fungi and significantly fewer gram+ bacteria in the 0-2 mm section than in those beyond 4 mm (Fig. 5d).

Fungi/bacteria ratios from total microbial PLFAs decreased between day 0 and day 3 before increasing again to reach values of  $0.029 \pm 0.043$  at pF 1.5,  $0.036 \pm 0.052$  at pF 2.5 and  $0.059 \pm 0.058$  at pF 3.5 after 45 days of incubation. The ratios were significantly higher at pF 3.5 than at pF 1.5 and pF 2.5 after 45 days of incubation. Finally, the fungi/bacteria ratios also evolved with the distance from residues and significantly decreased between the first two mm of soil ( $0.062 \pm 0.041$ ) and greater distances (with ratios from  $0.010 \pm 0.015$  to  $0.016 \pm 0.023$ ) (sup mat Figs. 5 and 6).

The fungi/bacteria ratios increased over time in the 0-2 mm section and were higher at pF 3.5 than at pF 1.5 after 45 days (sup mat Fig. 5). Beyond 2 mm, the ratios remained similar over time with no significant difference. However, the fungi/bacteria ratios in soil at distances  $>2$  mm from the residues were significantly higher at pF 3.5 than at pF 2.5 and 1.5, regardless of the incubation date (sup mat Fig. 6). These variations in the ratios between days 0 and 45 in



the first 2 mm of the soil were mainly due to an initial decrease and then significant increase in fungal PLFAs as well as a significant decrease in bacterial PLFAs (sup mat Fig. 7). Overall, the fungi/bacteria ratios were more dependent on the fungal marker content ( $R^2 = 0.86$ ) than on those of bacterial markers ( $R^2 = 0.04$ ).

### *3.5. Distribution of residue C-degrading microorganisms after 7 days of incubation*

After 7 days of incubation, total  $^{13}\text{C}$ -microbial PLFAs were similar between pF 1.5 and 3.5, but we observed some differences between pF 1.5 and 3.5 with more gram+ bacteria at pF 3.5 than 1.5 and conversely more gram- bacteria and fungi at pF 1.5 than 3.5, although none of the differences were significant. The fungi/bacteria ratios of  $^{13}\text{C}$ -PLFAs at the core scale were 0.096 at pF 1.5 and 0.037 at pF 3.5. The fungi/bacteria ratios of  $^{13}\text{C}$ -PLFAs were thus higher than the ratios calculated from total microbial PLFAs at pF 1.5 and similar to those at pF 3.5.

Total  $^{13}\text{C}$ -microbial PLFAs expressed in  $\text{nmol g}^{-1}$  were significantly more concentrated near the residues than at greater distances regardless of the matric potential but without a significant difference between pF 1.5 and 3.5 (Fig. 6). Thus, 75.4% and 88.0% of total  $^{13}\text{C}$ -microbial PLFAs were concentrated in the 0-2 mm section at pF 1.5 and 3.5, respectively, and 15.8% of total  $^{13}\text{C}$ -microbial PLFAs were present between 2 and 4 mm at pF 1.5 compared to only 8.7% at pF 3.5. The differences were mainly due to bacteria.

$^{13}\text{C}$ -microbial PLFAs represented a decreasing proportion of total microbial PLFAs with increasing distance from the residue layer, with  $19.4 \pm 2.0\%$  and  $13.3 \pm 4.4\%$  of the total microbial PLFAs for pF 1.5 and 3.5 at 0-2 mm,  $4.7 \pm 0.7\%$  and  $1.8 \pm 0.5\%$  at 2-4 mm,  $2.3 \pm 0.3\%$  and  $0.5 \pm 0.1\%$  at 4-6 mm and finally  $0.5 \pm 0.2\%$  and  $0.1 \pm 0.04\%$  at 12-14 mm, respectively. In the 0-2 mm zone,  $32.6 \pm 7.6\%$  of total fungi and  $16.8 \pm 1.5\%$  of total bacteria had assimilated

$^{13}\text{C}$  at pF 1.5 compared to  $15.5\pm 4.3\%$  of fungi and  $11.9\pm 4.4\%$  of bacteria at pF 3.5 (sup mat Fig. 8).

Comparing the microbial community structure of total and degrading microorganisms *via* PCA showed that these communities were clearly distinct, regardless of the matric potential (Fig. 7) and the distance to the residues (sup mat Fig. 10). Furthermore, the composition of microorganisms assimilating residue C were much less affected by soil moisture (Fig. 7) than that of the overall microbial community and much more affected by distance to the residues (sup mat Fig. 10).

#### 4. Discussion

##### 4.1. *Size of the detritosphere*

When quantifying  $^{13}\text{C}$  in the soil sections, we detected  $^{13}\text{C}$  up to 14 mm from the residues, but approximately 80% of the residue C present in soil was within the first 2 mm from the residues. Under diffusive conditions and based on  $^{13}\text{C}$  quantification, Gaillard et al. (1999) considered that the detritosphere was approximately 4 millimetres after the addition of wheat straw and 5 mm after the addition of young rye leaves, while Poll et al. (2006) measured a 1.6 mm thickness with maize residues, and Poll et al. (2008) measured 3 mm with rye residues (sup mat, Table 1). These differences likely result from the abundance of the soluble fraction of the residues, susceptibility to diffusion, soil structure and moisture conditions that affected the transfer of soluble C to the soil (diffusion, advection), fungi/bacteria balance and microbial activity. We confirmed that gradients of residue-derived C rapidly were established and persisted over several weeks.

#### 4.2. *Microbial communities in the detritosphere*

Regarding the total microbial community, we found that the 0-2 mm soil zone harboured a distinct microbial community structure with more fungi than the other soil zones. Thus, fungi/bacteria ratios decreased with increasing distance from the residues, as also observed by Poll et al. (2006) and Marschner et al. (2012). Microorganisms present in the 0-2 mm zone probably originated at least in part from the maize residues.

After 7 days of incubation, the  $^{13}\text{C}$  microbial community was distinct from the total microbial community and was composed of both bacteria and fungi (Fig. 7). These results are partly contradictory with previous works that showed that during the degradation of plant residues, bacteria were first involved in decomposition, and once soluble C had been assimilated, fungi took over to degrade more complex substrates such as hemicellulose and lignin (e.g., Marschner et al., 2011). Our results are nevertheless more consistent with those of Kramer et al. (2016), who showed that bacteria and fungi were able to degrade soluble  $^{13}\text{C}$  from plant residues and concluded that distinct bacterial and fungal energy channels were not apparent for labile versus recalcitrant substrates.

Thus, decomposition of residues in the adjacent soil certainly results from both soluble residue C diffusion and assimilation by soil microorganisms (Gaillard et al., 1999) and residue C translocation by fungi, especially in the case where fungi need N for residue decomposition (Frey et al., 2003). Degrading microorganisms were mainly concentrated near residues. In our experiment, the degrading microbial biomass (within 2 mm distance from the residues) represented 19% of the total microbial biomass at pF 1.5 and 13% at pF 3.5, which is consistent with Poll et al. (2006), who estimated the residue-degrading microbial biomass to be 5 to 20% of the total PLFAs at 1 mm from the residues. Gaillard et al. (1999) showed

that the microbial biomass involved in the degradation of wheat straw represented 12.5-20.4% of the total microbial biomass.

#### *4.3 Impact of matric potential on the detritosphere*

In our experiment, we considered a detritosphere functioning under different soil moistures, from pF 1.5, where pores with diameters up to 100  $\mu\text{m}$  were filled with water, to pF 3.5, where only pores of less than 1  $\mu\text{m}$  were water saturated. At pF 1.5, 80% of the total soil pore volume was filled with water, while at pF 3.5, only 23% of the total soil pore volume was filled with water. The detritosphere has not yet been studied under such dry conditions, and we expected to find more fungi at pF 3.5 than at other pF values, leading to an increase in the detritosphere size because of residue C translocation through fungal hyphae becoming the main transfer process.

From the start of the incubation, the mineralization of residue C was significantly larger at pF 1.5, when the soil was wet, than at pF 3.5 (Fig. 2 and 8). These results are consistent with the many experiments monitoring the mineralization of residues at different soil moistures when incorporated and mixed with soil (Moyano et al., 2012). The mineralization of residue C may occur on the residues themselves and in soil after the transfer of C from residues into soil, either by diffusion or by fungal translocation. Gaillard et al. (2003) showed that the residues themselves were the main sites of mineralization. Depending on litter quality, they found that in the short term, 24 to 33% of the residue C mineralization occurred in the soil, and 76 to 67% occurred on the residues themselves. Even if we did not directly measure the contribution of the two spatial compartments (residues and detritosphere soil) to the total mineralization, our results are consistent with those of Gaillard et al. (2003)

since we observed a strong correlation between the decrease in  $^{13}\text{C}$  in the residue layer and  $^{13}\text{C}$  mineralization (and not between  $^{13}\text{C}$  in soil and  $^{13}\text{C}$  mineralization). Furthermore, the quantity of degrading microorganisms detected in soil after 7 days (0.00003% of soil  $^{13}\text{C}$ ) was very low, suggesting that the microbial uptake of residue C and its mineralization in soil were small.

Nevertheless, we showed that a fraction of residue C was transferred into soil. C transport occurred early in the incubation, as previously observed by Gaillard et al. (1999) and Poll et al. (2006, 2008). The transfer of  $^{13}\text{C}$  into soil was dependent on the matric potential. Indeed, after 7 days, the transfer of  $^{13}\text{C}$  from residues into soil was significantly higher at pF 1.5 than at pF 3.5 (13 and 9% of added  $^{13}\text{C}$ , respectively) and was observed over longer distances (14 mm at pF 1.5 and between 6 and 12 mm at pF 3.5) (Fig. 5 and 8). Poll et al. (2006) observed that the amount of maize-derived C in the detritosphere was 55% higher in soil at pF 1.8 than at pF 2.5 and mainly concentrated within the first 1.2 mm from the residue layer. However, in our experiment, the transfer of  $^{13}\text{C}$  from the residues into soil under dry conditions reached the same distance as that under high-moisture conditions after 15 days. Thus, the detritosphere in the dry soil was of the same dimension as in the wet soil but appeared with a time lag. This result shows that the temporal pattern of C transport was impacted by the soil moisture.

Unexpectedly, the amounts of degrading microorganisms ( $^{13}\text{C}$  labelled) were low and similar at pF 1.5 and pF 3.5 after 7 days. These results are contradictory to those of Poll et al. (2006), who observed that more maize C was incorporated into PLFAs at pF 2.5 than at pF 1.8. In dry soil, there were fewer degrading fungi than in wet soil, while the analysis of total microbial PLFAs showed that the dry soil was, as expected, dominated by fungi and gram+ bacteria, which are more resistant to water stress than gram- bacteria. Furthermore, more bacteria had assimilated residue C between 2 and 4 mm at pF 1.5 than at 3.5, probably due to

a stronger and more distant diffusion of residue C, while fungi were only concentrated in the 0-2 mm zone. Hence, translocation of residue C by fungal hyphae seems negligible over distances larger than 2 mm. Thus, we assumed that under both low- and high-moisture conditions, the transport of residue C into the soil was mainly due to diffusion. Fungi assimilated residue C directly in the vicinity of the residues, while bacteria were more dependent on residue C transport in the adjacent soil. Therefore, the results of this study did not confirm our initial hypothesis on the role of fungi in dry soils.

In addition, the analysis of the microbial communities showed that the microorganisms involved in the degradation of residues ( $^{13}\text{C}$ -microbial PLFAs) were different from total microorganisms but similar at pF 1.5 and pF 3.5. Therefore, we assumed that carbon use efficiencies of degrading microorganisms located in the detritosphere soil were similar under the two studied moisture conditions and that residue C mineralization fluxes from soil after 7 days were small and equivalent regardless of matric potential.

The proportion of active microorganisms ( $^{13}\text{C}$ -PLFAs/total PLFAs) was nevertheless higher at pF 1.5 than at pF 3.5 (7% vs 4%), suggesting that an increased water content promoted accessibility and contact probabilities between microorganisms and the substrate.

## **5. Conclusion**

We found that the detritosphere constituted an area a few millimetres thick around decomposing residues, and most of the carbon transferred from the residues to the soil was found in the first 2 millimetres regardless of the soil moisture. Soil moisture still played a role in influencing the rates of transfer of residue C beyond this zone, but this effect remained minor, as only small amounts of residue C were transported beyond 2 mm. The drier the soil, the more abundant the fungi, but fungi were not the main organisms causing residue C

mineralization in the detritosphere soil. Most of the residue C mineralization took place on the residues themselves, at least in the first stages of decomposition, confirming that detritosphere hotspots represent a very small proportion of the soil volume, i.e., fresh residues and a few adjacent millimetres, where most of the microbial activity and biogeochemical processes took place.

### **Conflict of interest**

The authors declare that they have no known competing financial interests or personal relationships that could have appeared to influence the work reported in this paper.

### **Acknowledgements**

This work was supported by a grant from the French ANR to project Soil $\mu$ -3D (ANR-15-CE01-0006). We would like to thank the reviewers for their suggestions and constructive comments that have greatly improved the quality of the manuscript.

### **References**

- Autret, B., Mary, B., Chenu, C., Balabane, M., Girardin, C., Bertrand, M., Grandeau, G., Beaudoin, N., 2016. Alternative arable cropping systems: A key to increase soil organic carbon storage? Results from a 16 year field experiment. *Agriculture, Ecosystems & Environment* 232, 150–164. <https://doi.org/10.1016/j.agee.2016.07.008>
- Beare, M.H., Coleman, D.C., Crossley Jr, D.A., Hendrix, P.F., Odum, E.P., 1995. A hierarchical approach to evaluating the significance of soil biodiversity to biogeochemical cycling. *Plant and Soil* 170, 5–22.
- Chenu, C., J., H., J., B., 2001. Short-term changes in the spatial distribution of microorganisms in soil aggregates as affected by glucose addition. *Biology and Fertility of Soils* 34, 349–356. <https://doi.org/10.1007/s003740100419>

- Chenu, C., Plante, A.F., 2006. Clay-sized organo-mineral complexes in a cultivation chronosequence: revisiting the concept of the “primary organo-mineral complex.” *European Journal of Soil Science* 57, 596–607. <https://doi.org/10.1111/j.1365-2389.2006.00834.x>
- Chenu, C., Stotzky, G., 2002. Interaction between microorganisms and soil particles: an overview, in: Huang, P.M., Bollag, P.M., Senesi, N. (Eds.), *Interaction between Soil Particles and Microorganisms. Impact on the Terrestrial Ecosystem*, IUPAC Series on Analytical and Physical Chemistry of Environmental Systems. John Wiley & Sons, New York, pp. 3–40.
- Chowdhury, N., Marschner, P., Burns, R., 2011. Response of microbial activity and community structure to decreasing soil osmotic and matric potential. *Plant and Soil* 344, 241–254. <https://doi.org/10.1007/s11104-011-0743-9>
- Ekschmitt, K., Kandeler, E., Poll, C., Brune, A., Buscot, F., Friedrich, M., Gleixner, G., Hartmann, A., Kästner, M., Marhan, S., Miltner, A., Scheu, S., Wolters, V., 2008. Soil-carbon preservation through habitat constraints and biological limitations on decomposer activity. *Journal of Plant Nutrition and Soil Science* 171, 27–35. <https://doi.org/10.1002/jpln.200700051>
- Frey, S.D., Six, J., Elliott, E.T., 2003. Reciprocal transfer of carbon and nitrogen by decomposer fungi at the soil–litter interface. *Soil Biology and Biochemistry* 35, 1001–1004. [https://doi.org/10.1016/S0038-0717\(03\)00155-X](https://doi.org/10.1016/S0038-0717(03)00155-X)
- Frostegård, Å., E. Bååth, A. Tunlio, 1993. Shifts in the structure of soil microbial communities in limed forest as revealed by phospholipid fatty acid analysis. *Soil Biology and Biochemistry* 25, 723–730.
- Gaillard, V., Chenu, C., Recous, S., 2003. Carbon mineralisation in soil adjacent to plant residues of contrasting biochemical quality. *Soil biology and biochemistry* 35, 93–99.
- Gaillard, V., Chenu, C., Recous, S., Richard, G., 1999. Carbon, nitrogen and microbial gradients induced by plant residues decomposing in soil. *European Journal of Soil Science* 50, 567–578.
- Kandeler, E., 1999. Xylanase, invertase and protease at the soil–litter interface of a loamy sand. *Soil Biology and Biochemistry* 31, 1171–1179. [https://doi.org/10.1016/S0038-0717\(99\)00035-8](https://doi.org/10.1016/S0038-0717(99)00035-8)
- Klute, A., 1986. Water Retention: Laboratory Methods, in: Klute, Arnold (Ed.), *SSSA Book Series*. Soil Science Society of America, American Society of Agronomy, Madison, WI, USA, pp. 635–662. <https://doi.org/10.2136/sssabookser5.1.2ed.c26>



- Kramer, S., Dibbern, D., Moll, J., Huenninghaus, M., Koller, R., Krueger, D., Marhan, S., Urich, T., Wubet, T., Bonkowski, M., Buscot, F., Lueders, T., Kandeler, E., 2016. Resource Partitioning between Bacteria, Fungi, and Protists in the Detritosphere of an Agricultural Soil. *Frontiers in Microbiology* 7, 1–12. <https://doi.org/10.3389/fmicb.2016.01524>
- Kuzyakov, Y., Blagodatskaya, E., 2015. Microbial hotspots and hot moments in soil: Concept & review. *Soil Biology and Biochemistry* 83, 184–199. <https://doi.org/10.1016/j.soilbio.2015.01.025>
- Lerch, T.Z., Dignac, M.-F., Nunan, N., Bardoux, G., Barriuso, E., Mariotti, A., 2009. Dynamics of soil microbial populations involved in 2,4-D biodegradation revealed by FAME-based Stable Isotope Probing. *Soil Biology and Biochemistry* 41, 77–85. <https://doi.org/10.1016/j.soilbio.2008.09.020>
- Marschner, P., Marhan, S., Kandeler, E., 2012. Microscale distribution and function of soil microorganisms in the interface between rhizosphere and detritosphere. *Soil Biology and Biochemistry* 49, 174–183. <https://doi.org/10.1016/j.soilbio.2012.01.033>
- Marschner, P., Umar, S., Baumann, K., 2011. The microbial community composition changes rapidly in the early stages of decomposition of wheat residue. *Soil Biology and Biochemistry* 43, 445–451. <https://doi.org/10.1016/j.soilbio.2010.11.015>
- Monga, O., Garnier, P., Pot, V., Coucheney, E., Nunan, N., Otten, W., Chenu, C., 2014. Simulating microbial degradation of organic matter in a simple porous system using the 3-D diffusion-based model MOSAIC. *Biogeosciences* 11, 2201–2209. <https://doi.org/10.5194/bg-11-2201-2014>
- Moyano, F.E., Manzoni, S., Chenu, C., 2013. Responses of soil heterotrophic respiration to moisture availability: An exploration of processes and models. *Soil Biology and Biochemistry* 59, 72–85. <https://doi.org/10.1016/j.soilbio.2013.01.002>
- Moyano, F.E., Vasilyeva, N., Bouckaert, L., Cook, F., Craine, J., Curiel Yuste, J., Don, A., Epron, D., Formanek, P., Franzluebbers, A., Ilstedt, U., Kätterer, T., Orchard, V., Reichstein, M., Rey, A., Ruamps, L., Subke, J.-A., Thomsen, I.K., Chenu, C., 2012. The moisture response of soil heterotrophic respiration: interaction with soil properties. *Biogeosciences* 9, 1173–1182. <https://doi.org/10.5194/bg-9-1173-2012>
- Peth, S., Chenu, C., Leblond, N., Mordhorst, A., Garnier, P., Nunan, N., Pot, V., Ogurreck, M., Beckmann, F., 2014. Localization of soil organic matter in soil aggregates using synchrotron-based X-ray microtomography. *Soil Biology and Biochemistry* 78, 189–194. <https://doi.org/10.1016/j.soilbio.2014.07.024>

- Pinheiro, M., Garnier, P., Beguet, J., Martin Laurent, F., Vieublé Gonod, L., 2015. The millimetre-scale distribution of 2,4-D and its degraders drives the fate of 2,4-D at the soil core scale. *Soil Biology and Biochemistry* 88, 90–100. <https://doi.org/10.1016/j.soilbio.2015.05.008>
- Pinheiro, M., Pagel, H., Poll, C., Ditterich, F., Garnier, P., Streck, T., Kandeler, E., Vieublé Gonod, L., 2018. Water flow drives small scale biogeography of pesticides and bacterial pesticide degraders - A microcosm study using 2,4-D as a model compound. *Soil Biology and Biochemistry* 127, 137–147. <https://doi.org/10.1016/j.soilbio.2018.09.024>
- Poll, C., Ingwersen, J., Stemmer, M., Gerzabek, M.H., Kandeler, E., 2006. Mechanisms of solute transport affect small-scale abundance and function of soil microorganisms in the detritosphere. *European Journal of Soil Science* 57, 583–595. <https://doi.org/10.1111/j.1365-2389.2006.00835.x>
- Poll, C., Marhan, S., Ingwersen, J., Kandeler, E., 2008. Dynamics of litter carbon turnover and microbial abundance in a rye detritosphere. *Soil Biology and Biochemistry* 40, 1306–1321. <https://doi.org/10.1016/j.soilbio.2007.04.002>
- Portell, X., Pot, V., Garnier, P., Otten, W., Baveye, P.C., 2018. Microscale Heterogeneity of the Spatial Distribution of Organic Matter Can Promote Bacterial Biodiversity in Soils: Insights From Computer Simulations. *Frontiers in Microbiology* 9. <https://doi.org/10.3389/fmicb.2018.01583>
- Quideau, S.A., McIntosh, A.C.S., Norris, C.E., Lloret, E., Swallow, M.J.B., Hannam, K., 2016. Extraction and Analysis of Microbial Phospholipid Fatty Acids in Soils. *Journal of Visualized Experiments* e543360. <https://doi.org/10.3791/54360>
- Ranjard, L., Richaume, A., 2001. Quantitative and qualitative microscale distribution of bacteria in soil. *Research in Microbiology* 152, 707–716.
- Raynaud, X., Nunan, N., 2014. Spatial Ecology of Bacteria at the Microscale in Soil. *PLoS ONE* 9, e87217. <https://doi.org/10.1371/journal.pone.0087217>
- Reichardt, W., Briones, A., de Jesus, R., Padre, B., 2001. Microbial population shifts in experimental rice systems. *Applied Soil Ecology* 17, 151–163. [https://doi.org/10.1016/S0929-1393\(01\)00122-6](https://doi.org/10.1016/S0929-1393(01)00122-6)
- Vogel, H.-J., Roth, K., 2001. Quantitative morphology and network representation of soil pore structure. *Advances in Water Resources* 24, 233–242. [https://doi.org/10.1016/S0309-1708\(00\)00055-5](https://doi.org/10.1016/S0309-1708(00)00055-5)



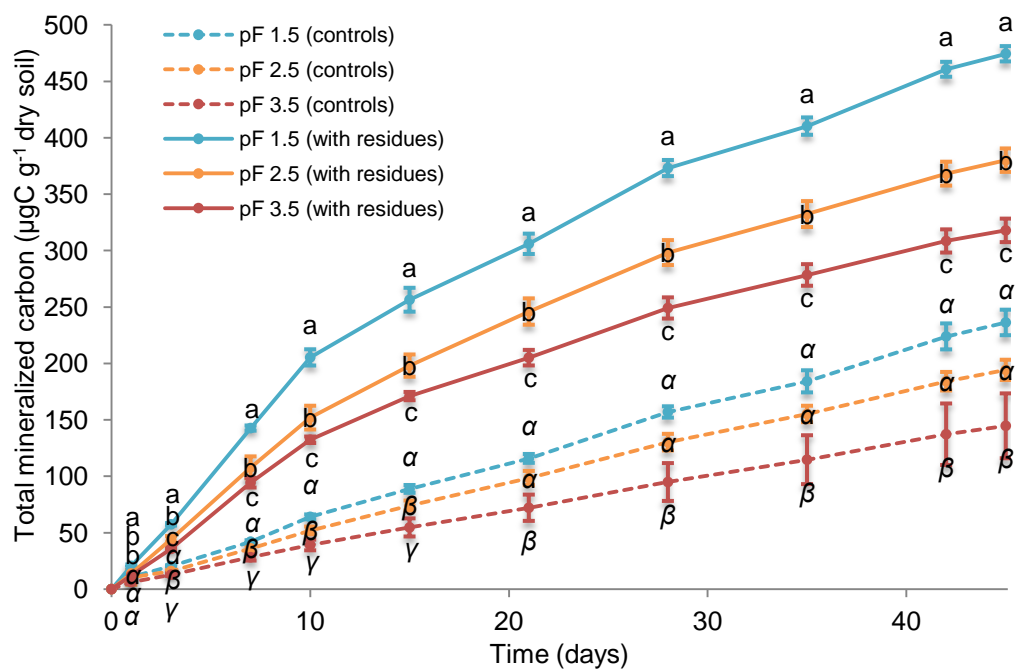
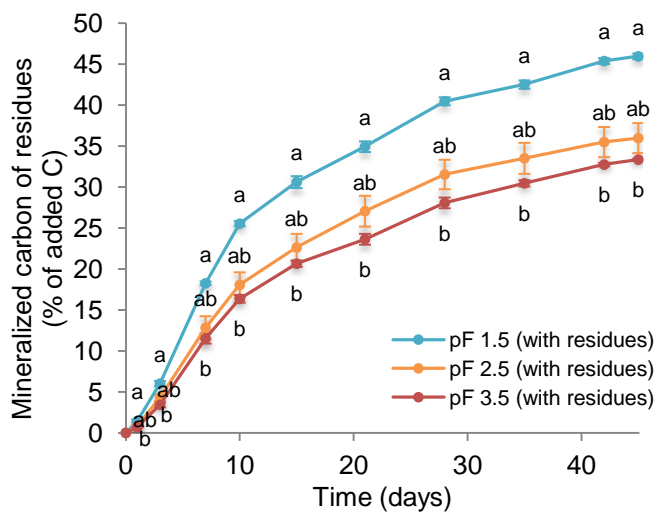
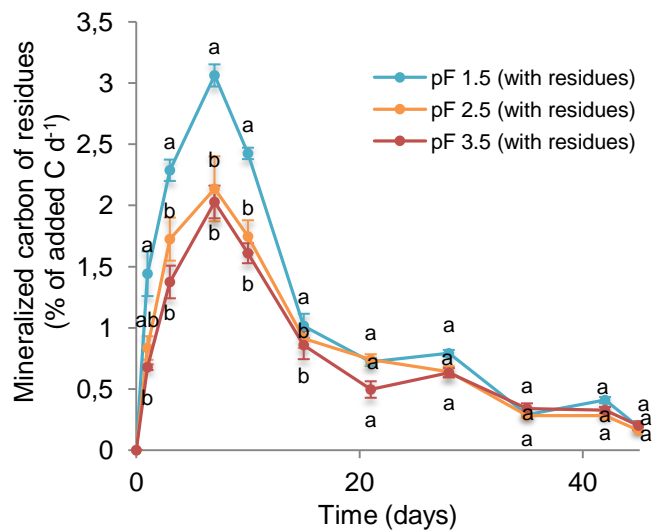


**Fig. 1.** Kinetics of total carbon mineralization of control soil and soil amended with residues over 45 days. The bars correspond to the standard deviation of the 3 replicates and the letters to the results of the statistical tests (Tukey test) between the 3 pFs for each date and each treatment (controls and amended cores treated separately).



(a)



(b)

**Fig. 2.** Kinetics of residues carbon mineralization: cumulative mineralization (a) and daily mineralization (b). In both cases, the bars correspond to the standard deviation of the replicates and the letters to the results of the statistical tests (Dunn test (a) and Tukey test (b)) between the 3 pFs for each date.

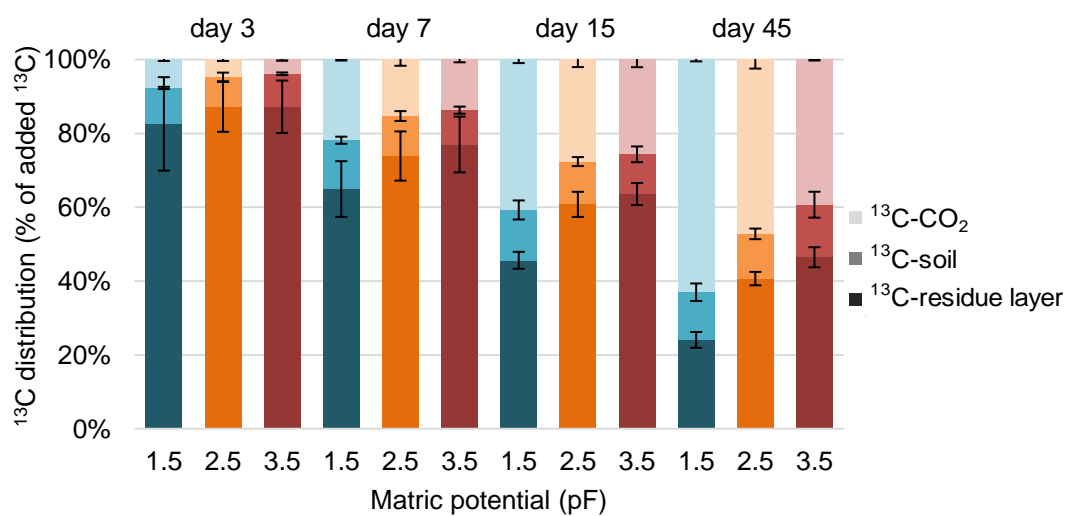


**Fig. 3.**  $^{13}\text{C}$  distribution (% of the added  $^{13}\text{C}$ ) in the mineralized, soil and residues fractions after 3, 7, 15 and 45 days of incubation for the 3 matric potentials.

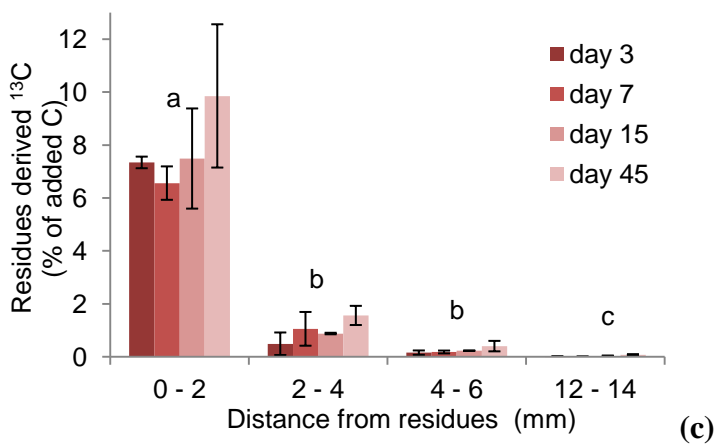
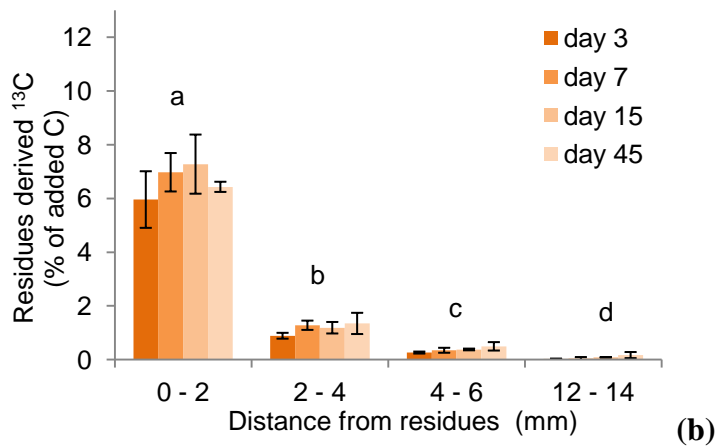
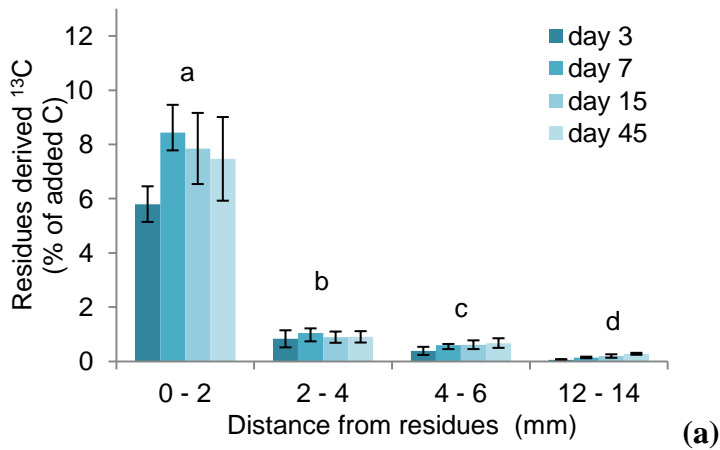


**Fig. 4.**  $^{13}\text{C}$  content from residues in different soil slices located at increasing distances from the residues layer (0-2, 2-4, 4-6 and 12-14 mm) after 3, 7, 15 and 45 days of incubation at pF1.5 (a), pF2.5 (b) and pF3.5 (c). The bars correspond to the standard deviation of the replicates and the letters to the results of the statistical tests (Dunn test) between slices 0-2, 2-4, 4-6 and 12-14 mm (all dates combined).

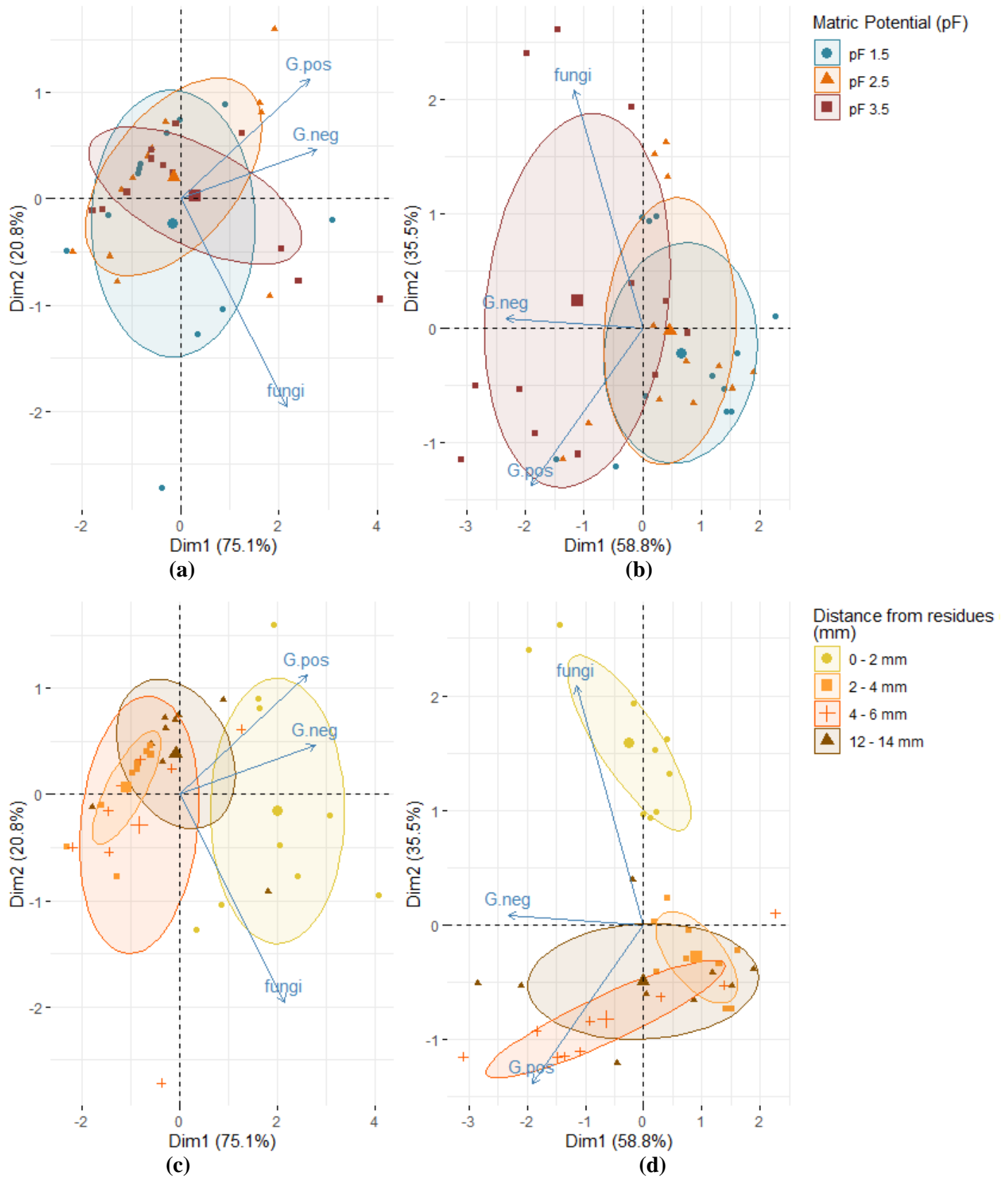


**Fig. 5.** Principal Component Analysis (PCA) of total microbial PLFAs corresponding to Gram-negative bacteria (G.neg), Gram-positive bacteria (G.pos) and fungi after 3 days (a, c) and 45 days (b, d) of incubation according to the 3 different matric potentials (a, b) and according to different slices of soil located at increasing distances from the residues (c, d).



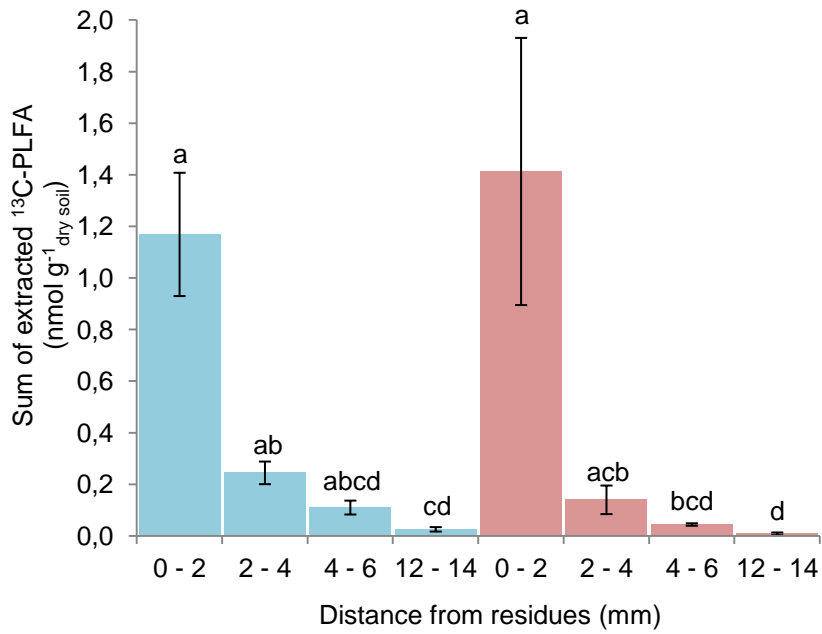


**Fig. 6.** <sup>13</sup>C-PLFA content according to different soil slices located at increasing distances from the residues (0-2, 2-4, 4-6 and 12-14 mm) at pF1.5 (blue) and 3.5 (red) after 7 days of incubation. The letters correspond to the results of the statistical tests (Dunn test).

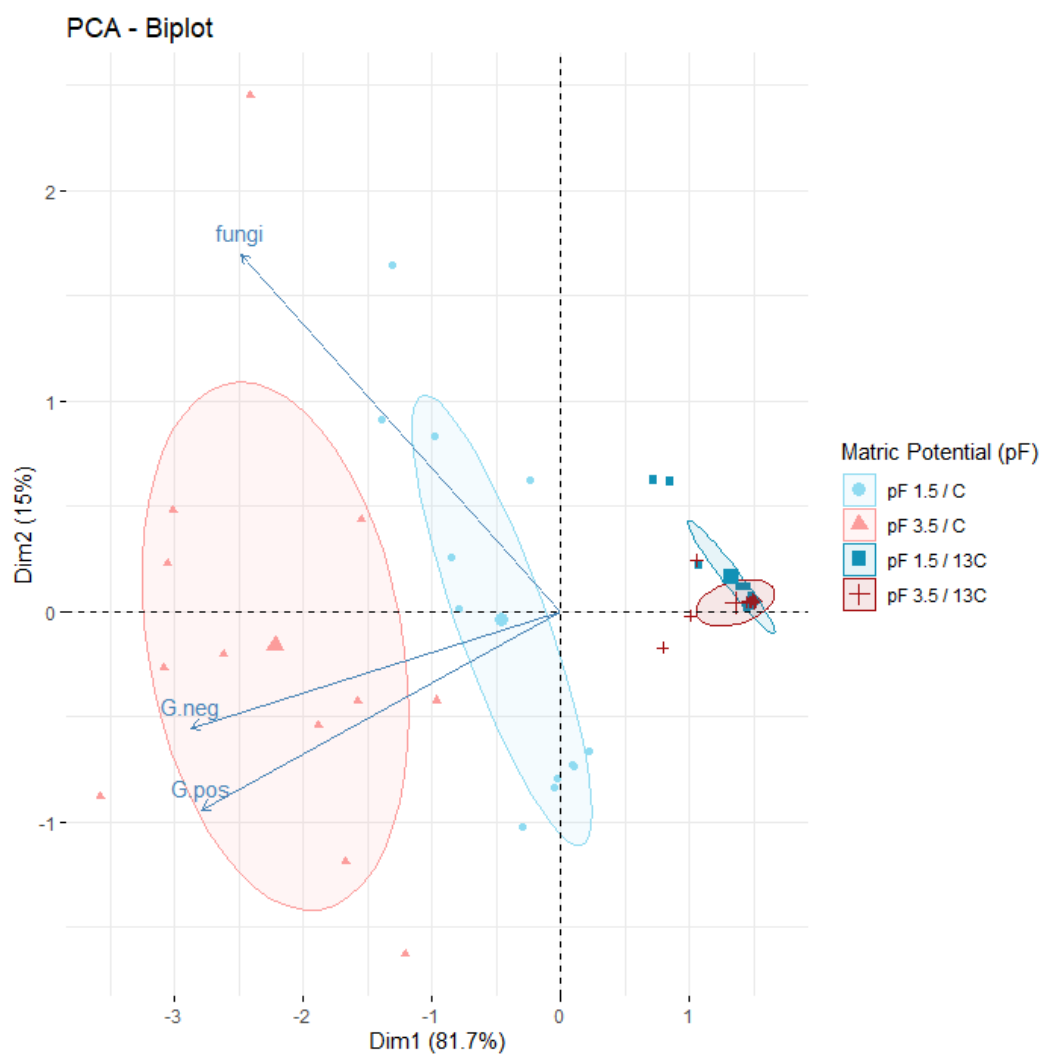


**Fig. 7.** Principal Component Analysis (PCA) of total PLFAs and <sup>13</sup>PLFAs according to matric potentials

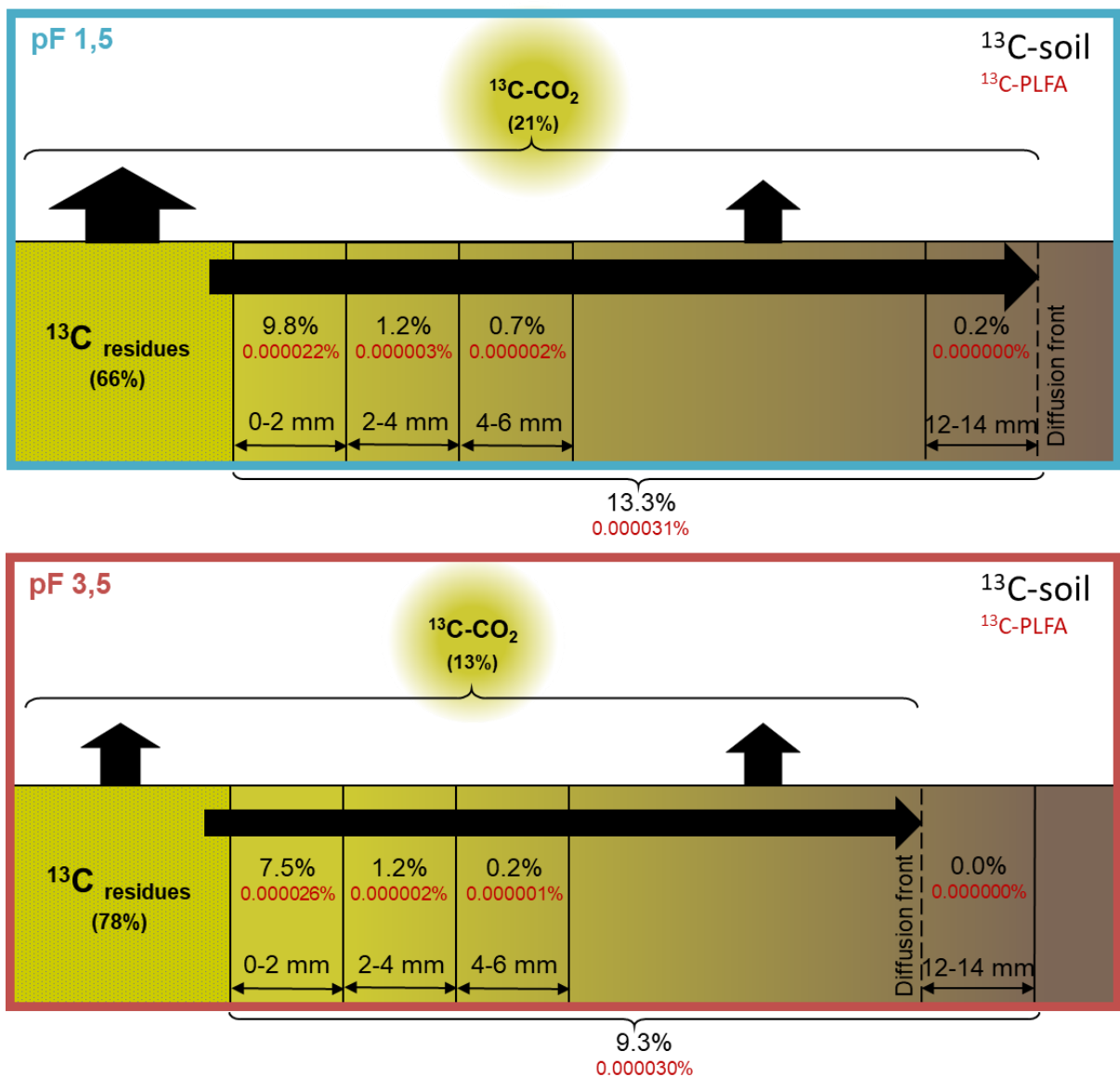


**Fig. 8.** Distribution of residue C in different spatial compartments after incubation of maize inflorescence for 7 days at pF 1.5 (on top) and 3.5 (on bottom), expressed in percentages of initial  $^{13}\text{C}$

## Supplementary materials

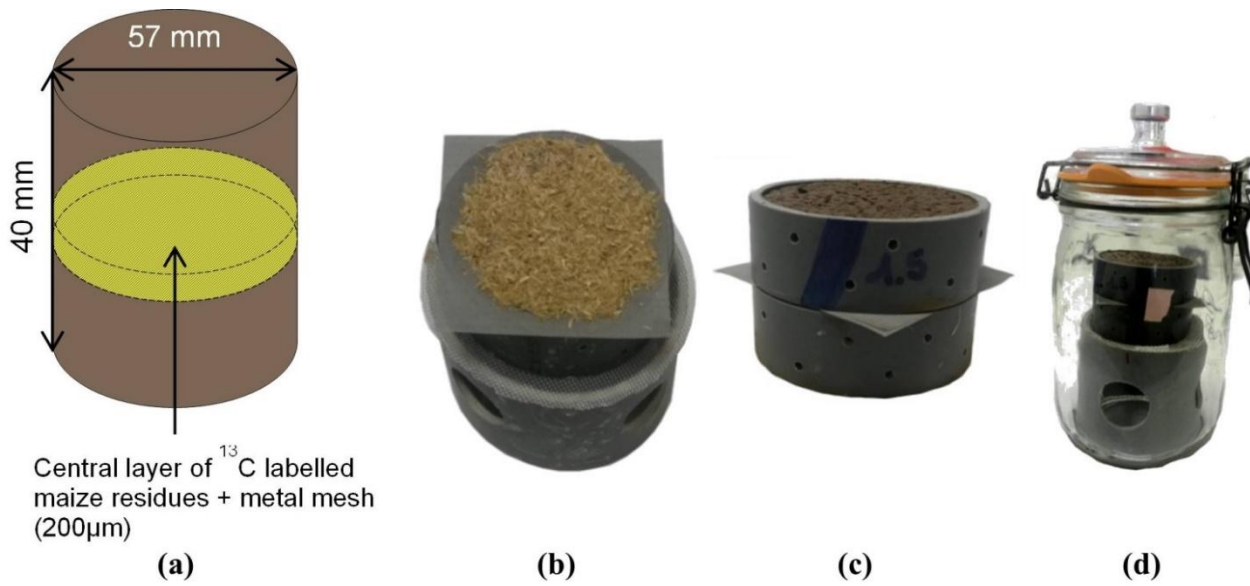


**Fig. S.1.** Construction of a soil core (a). Application of residues on the mesh (b). A core after construction (c). A core in its closed jar ready for incubation (d)

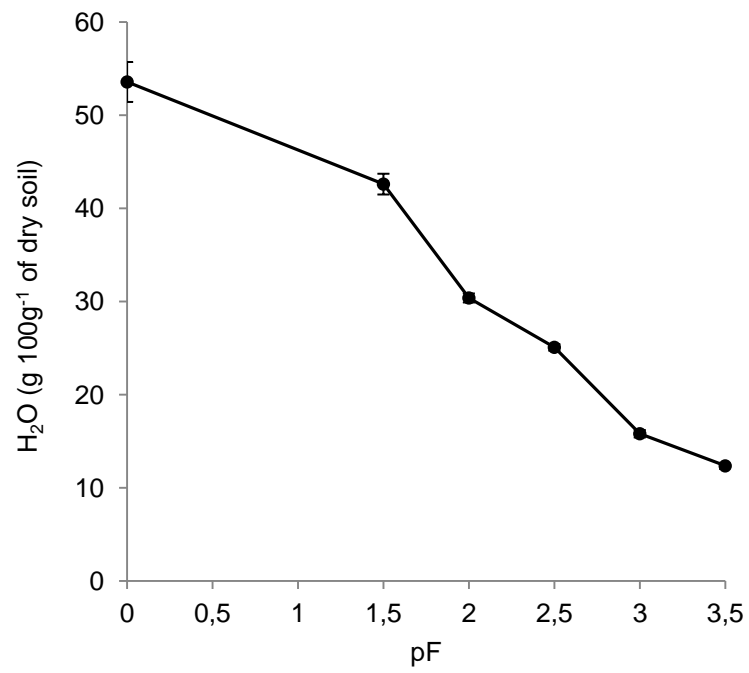


**Fig. S.2.** Water retention curve of the studied soil (n=3) ( $pF = -\log h$  where  $h$  is the pressure applied in water cm).

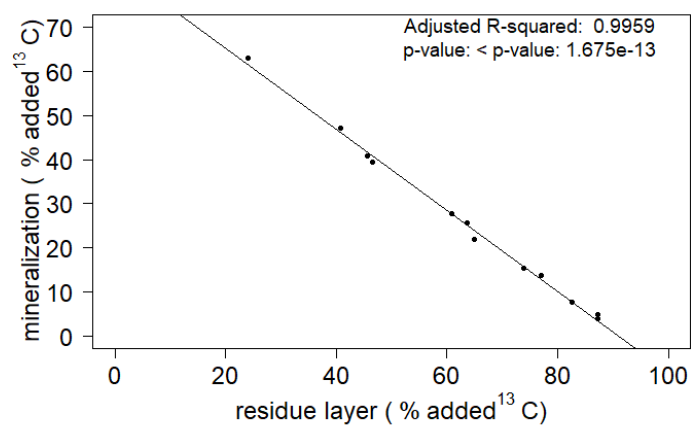


**Fig. S.3.** Correlations between  $^{13}\text{C}$  in the residue layer and mineralized  $^{13}\text{C}$

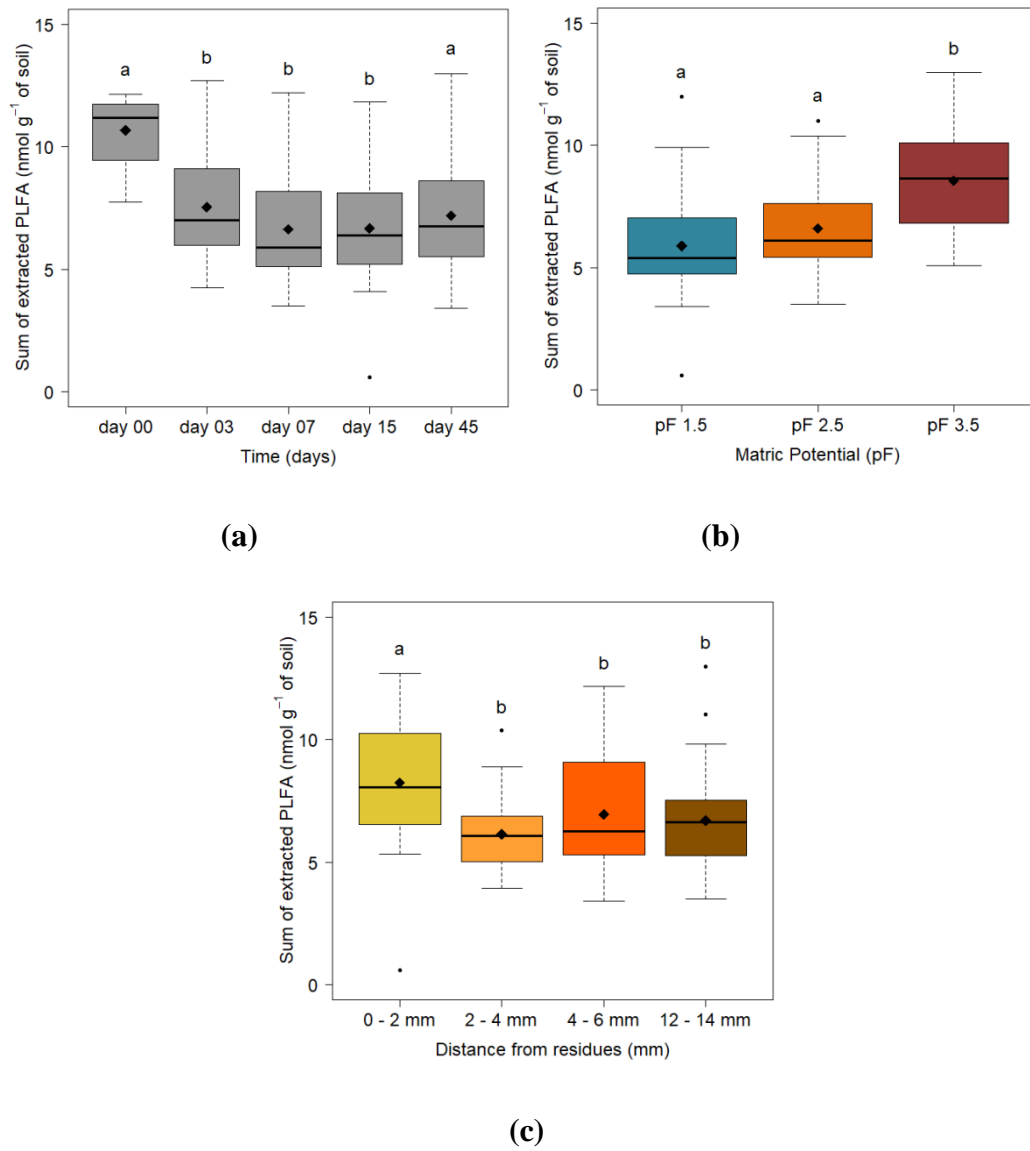


**Fig. S.4.** Total microbial PLFAs - all treatments combined - according to the different sampling dates (a), the different pFs (b) and the distances from residues (c). Black diamonds correspond to the means and the letters to the results of the statistical tests (Dunn test).

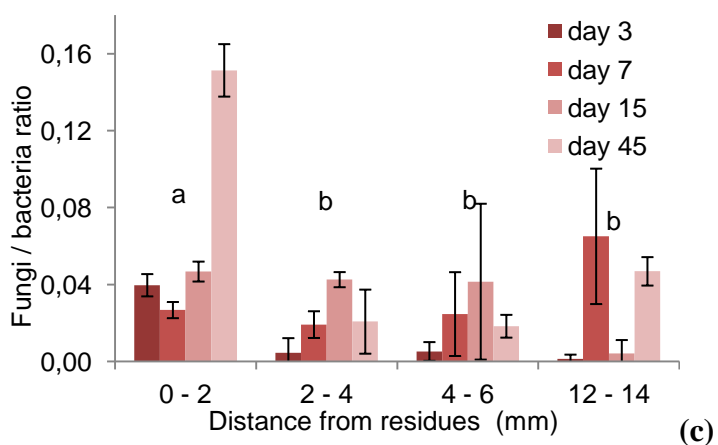
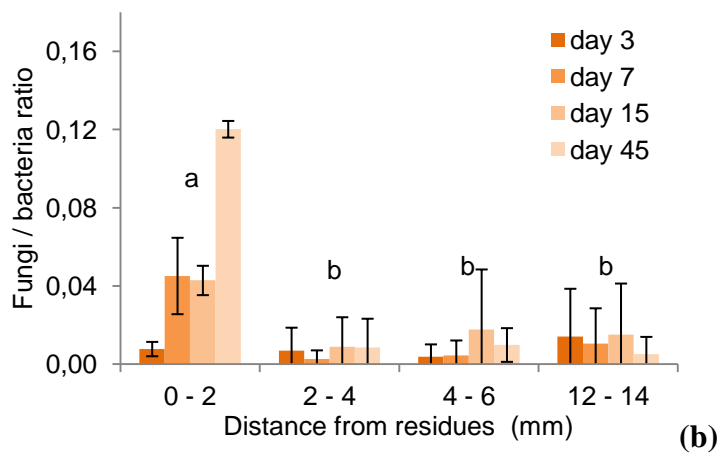
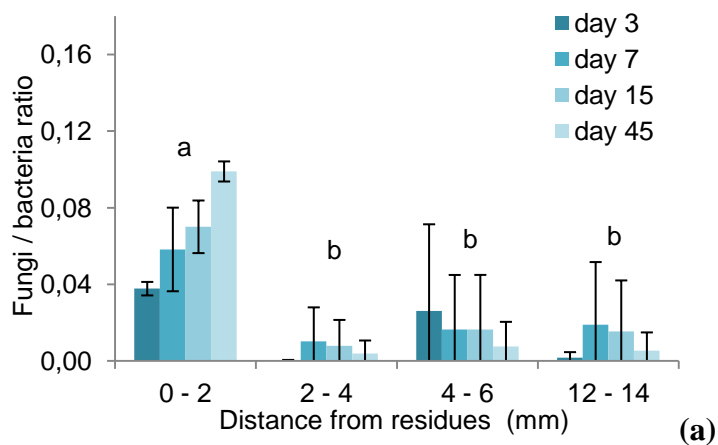
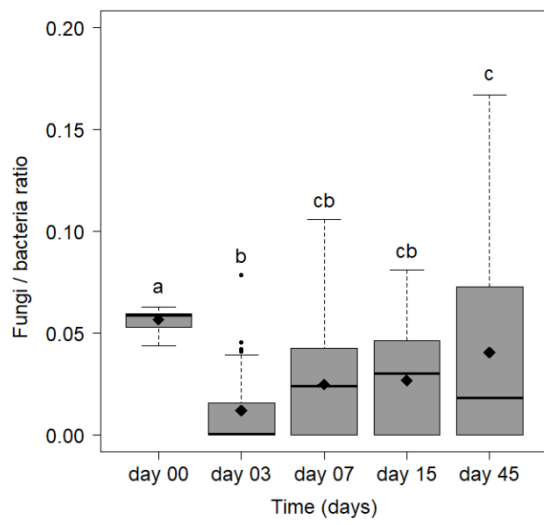
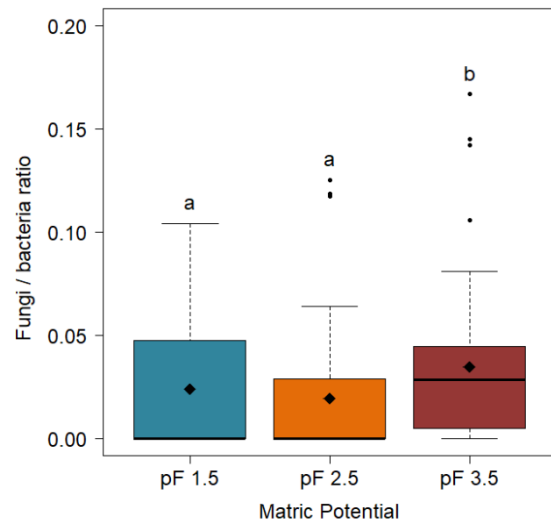


**Fig. S.5.** Evolution of the fungi/bacteria ratios in different soil slices located at increasing distances from the residue layer (0-2, 2-4, 4-6 and 12-14 mm) after 3, 7, 15 and 45 days of incubation at pF 1.5 (a), pF 2.5 (b) and pF 3.5 (c). The bars correspond to the standard deviation of the replicates and the letters to the results of the statistical tests (Dunn test) between slices 0-2, 2-4, 4-6 and 12-14 mm (all dates combined).

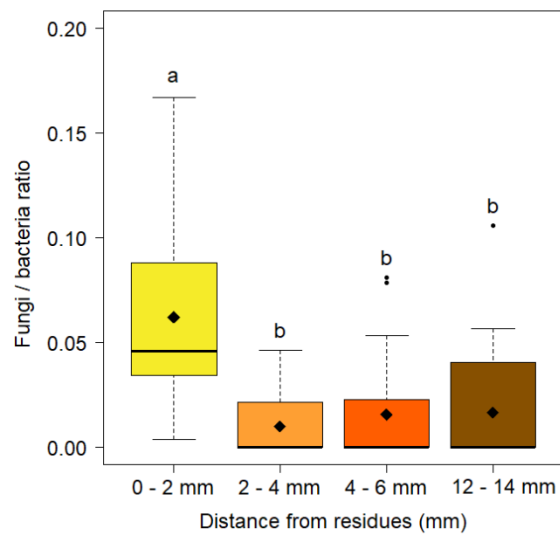




(a)



(b)



(c)

**Fig. S.6.** Fungi/bacteria ratios, all treatments combined, according to the different sampling dates (a), the different pFs (b) and the distances from residues (c). Black diamonds correspond to the means and the letters to the results of the statistical tests (Dunn test).

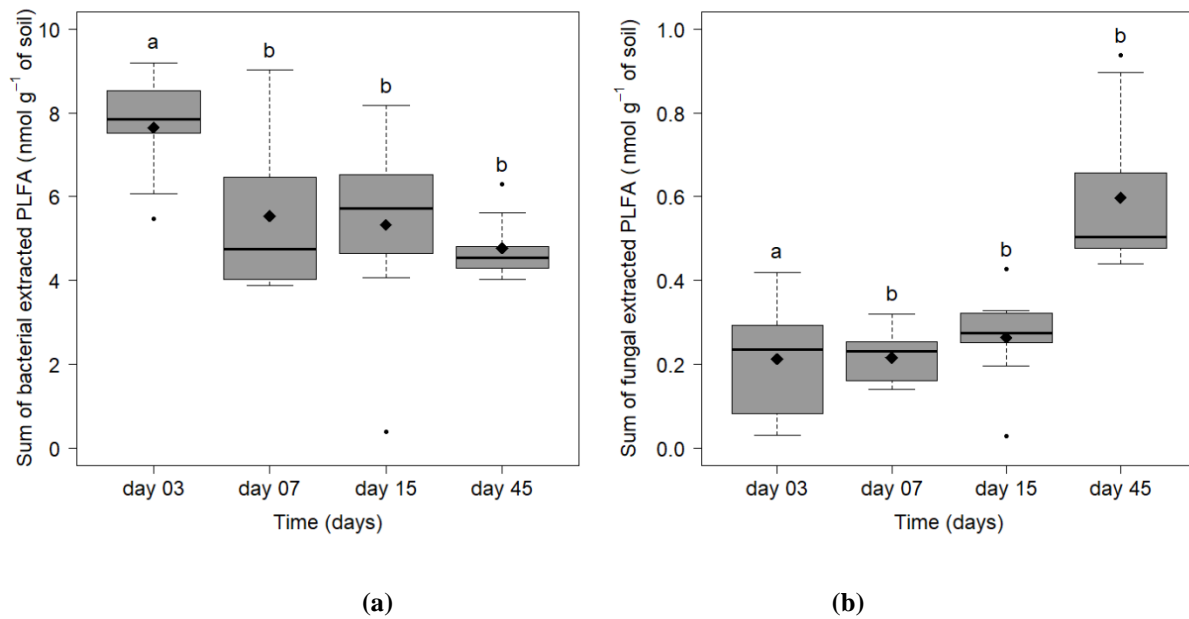
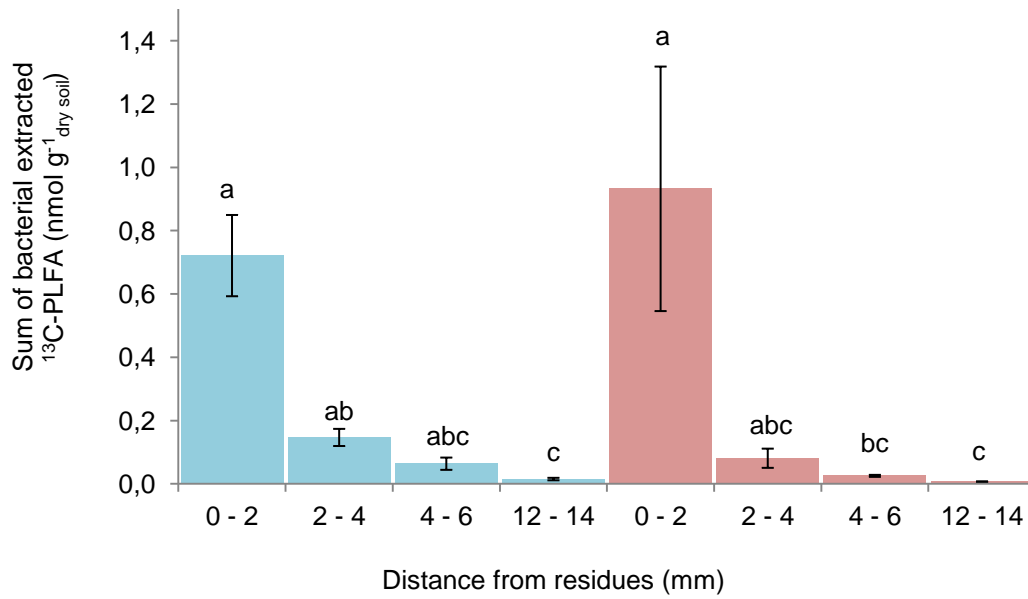
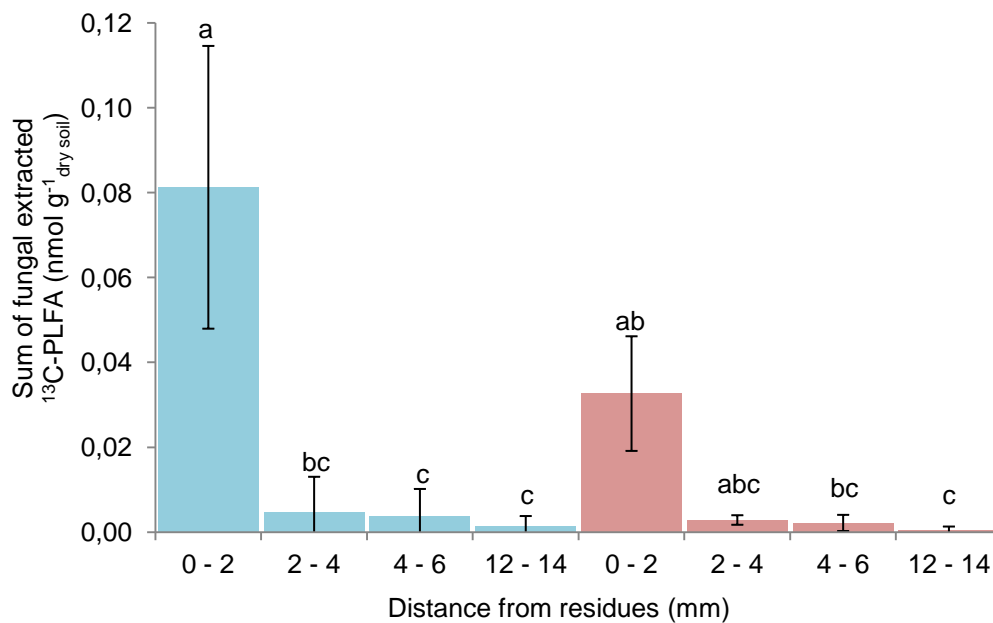


**Fig. S.7.** Bacterial (a) and fungal (b) PLFAs contents in the 2 first mm of soil, all matric potentials combined, and according to the different sampling dates. Black diamonds correspond to the means and the letters to the results of the statistical tests (Dunn test).

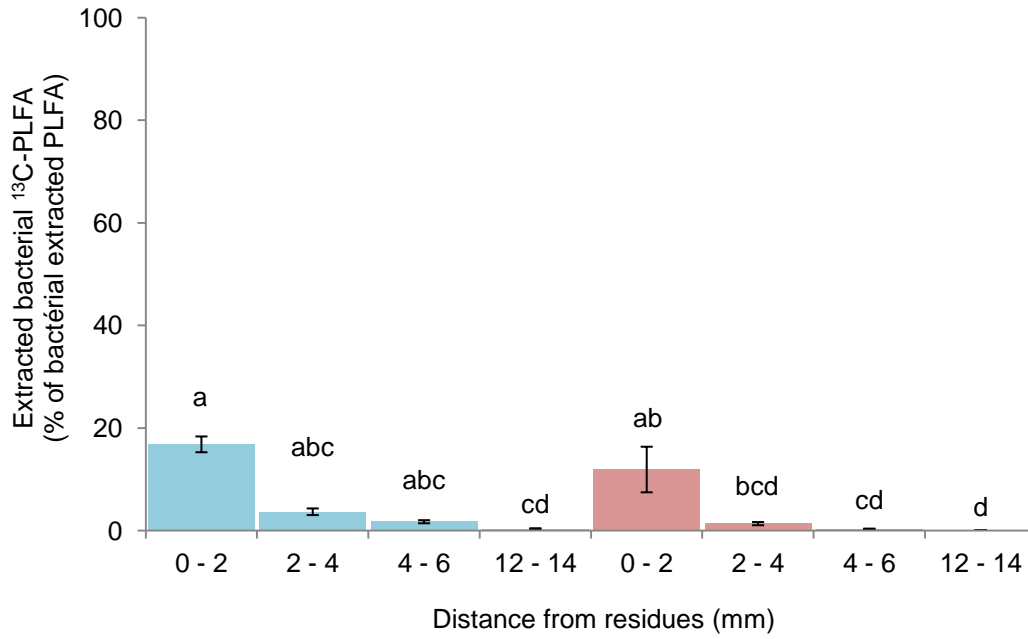


(a)

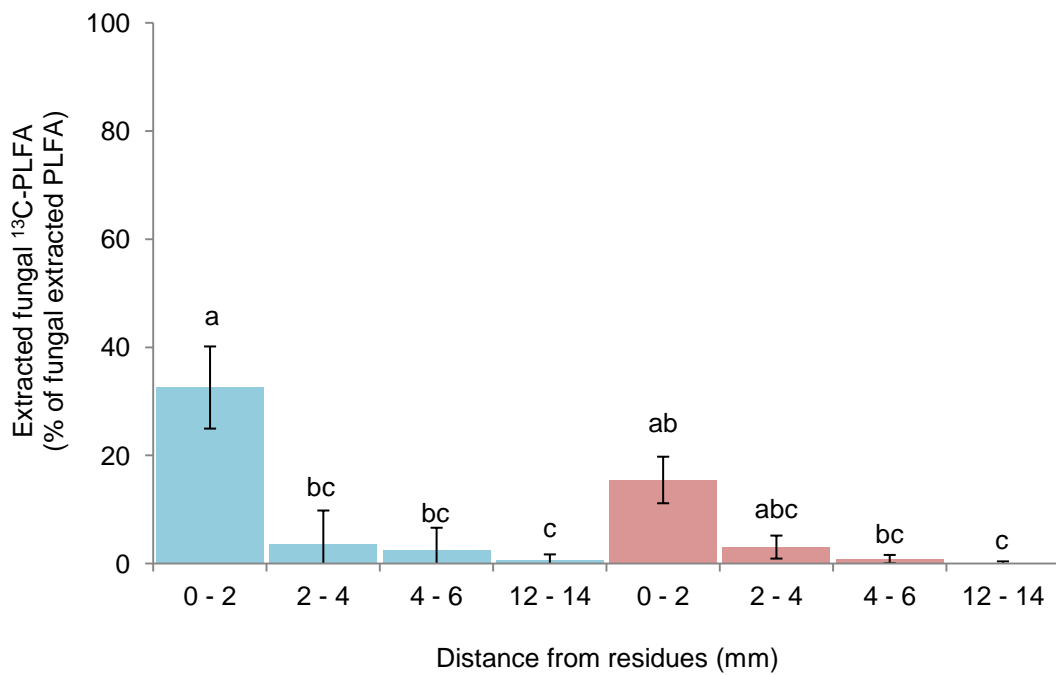


(b)

**Fig. S.8.** Bacterial (a) and fungal (b)  $^{13}\text{C}$ -PLFAs contents in different soil slices located at increasing distances from the residues (0-2, 2-4, 4-6 and 12-14 mm) at pF 1.5 (blue) and 3.5 (red) after 7 days of incubation. The letters correspond to the results of the statistical tests (Dunn test).



(a)



(b)

**Fig. S.9.** Percentage of bacterial (a) and fungal (b) <sup>13</sup>C-PLFAs contents expressed in % of total PLFAs in different soil slices located at increasing distances from the residues (0-2, 2-4, 4-6 and 12-14 mm) at pF 1.5 (blue) and 3.5 (red) after 7 days of incubation. The letters correspond to the results of the statistical tests (Dunn test).

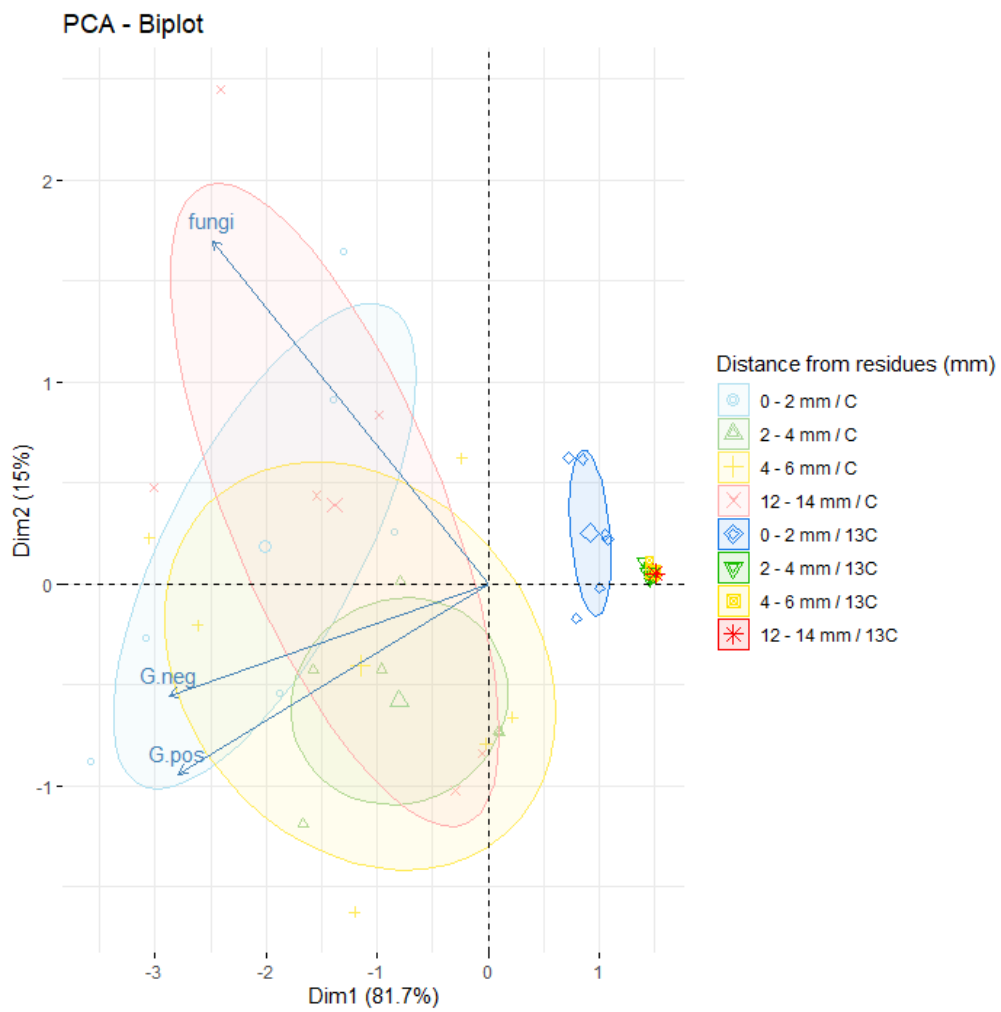


**Fig. S.10.** Principal Component Analysis (PCA) of total PLFAs and <sup>13</sup>C-PLFAs according to distances from the residues layer

**Table 1.** Size and microbial community evolution of detritusphere according to various incubation set-ups.

Soil	Residues	C:N / soluble C (% residue) / soluble fraction (% residue)	Matric potential (pF)	Temperatur e (°C)	Incubati on time (days)	Soil analyses	Detritusphe re size (mm)	Reference
Orthic luvisol	Mature wheat straw	166 / 5 / -	pF2.9	15	100	SOC, <sup>13</sup> C-SOC, DOC <sup>13</sup> C-DOC, microbial biomass, <sup>13</sup> C-microbial biomass and deshydrogenase activity	3-4	Gaillard et al. (1999)
Sandy loam	Maize straw	- / - / -	-	9	27	DOC and enzymes	1-2	Kandeler (1999)
Eutric cambisol	Mature wheat straw	167 / 5 / 17	pF2.2	15	10	CO <sub>2</sub> and <sup>13</sup> CO <sub>2</sub>	4-5	Gaillard et al. (2003)
	Young rye leaves	09 / 10 / 52			3		5-6	
Typic Fluvaquent	Rice straw	26 / 9 / -	pF2.0	25	30	SON, inorganic N and microbial biomass N	<2 / >10	Moritsuka et al. (2004)
	Rice bran	19 / 15 / -					<2 / >10	
	Beech leaves	46 / 7 / -					<2 / >10	
Woodburn silty loam	Unleached ryegrass straw	- / - / -	-	25	80	PLFA	-	McMahon et al. (2005)
	Leached ryegrass straw							
	Ryegrass leachate							
Stagnic luvisol	Maize leafs and stems	- / - / -	pF1.8	10	14	SOC, <sup>13</sup> C-SOC, PLFA, <sup>13</sup> C-PLFA, and enzymes	1.5–2.8	Poll et al. (2006)
			pF2.5				1.5–2.8	
			pF1.8 advection				2.5–3.0	
			pF2.5 advection				2.5–3.0	
Orthic luvisol	Mature wheat straw	66 / 5 / 23	pF2.7	15	168	SOC, <sup>13</sup> C-SOC, inorganic N, microbial biomass, <sup>13</sup> C-microbial biomass,	-	Nicolardot et al. (2007)
	Young rye leaves	21 / 17 / 53						
Stagnic luvisol	Rye	40 / - / -	pF1.8	10	84	SOC, <sup>13</sup> C-SOC, DOC <sup>13</sup> C-DOC, microbial biomass, <sup>13</sup> C-microbial biomass, ergosterol and enzymes	>3	Poll et al. (2008)
			pF2.5				>3	
Orthic luvisol	Mature wheat	- / - / -	pF2.7	15	168	16S and 18S rDNA	-	Bastian et al. (2009)
Orthic luvisol	Wheat	- / - / -	Field condition	Field condition	244	inorganic N, microbial biomass and 16S rRNA,	-	Pascault et al. (2010)
Quartz sand	wheat residue	- / 1.6 / -	-	22-25	30	PLFA	-	Marschner et al.

								(2011)
Chernozem	Mature wheat	74 / 2.3 / -	-	20	23	Inorganic N, PLFA, <sup>13</sup> C-PLFA, fungal PLFA, bacterial PLFA and enzymes	4 / >5	Marschner et al. (2012)
Cambisol/Luvisol/Stagnic luvisol	Maize leaves	- / - / -	-	12	32	CO <sub>2</sub> , <sup>13</sup> CO <sub>2</sub> , PLFA, <sup>13</sup> C-PLFA, rRNA and <sup>13</sup> C-rRNA	-	Kramer et al. (2016)
	Maize roots							
Luvisol/Cambisol	Senescent maize leaves	- / - / -	pF1.8	20	60	SOC, extractable organic C, microbial C and PLFA	-	Müller et al. (2017)
Luvisol	Maize inflorescence	20 / - / 23	pF1.5	20	50	SOC, <sup>13</sup> C-SOC, PLFA and <sup>13</sup> C-PLFA	2	Védère et al. this study
			pF2.5				2	
			pF3.5				2	